地質学論集　第52号　287-302ページ，1999年9月
Mem. Geol. Soc. Japan, No. 52, p. 287-302, September 1999

Petrogenesis of the Fuko Pass high-pressure metacumulate from the Oeyama peridotite body, southwestern Japan: evidence for Early Paleozoic subduction metamorphism

Tatsuki Tsujimori *

Received July 21, 1998.
Accepted May 27, 1999.
* Department of Earth Sciences, Faculty of Science, Kanazawa University, Kanazawa 920-1192, Japan

Abstract

The kyanite-bearing epidote-amphibolite originated in troctolitic cumulate rock, here defined as "Fuko Pass metacumulate", occurs as a fault-bounded block in the Oeyama peridotite body. The Fuko Pass metacumulate is variously deformed and thoroughly recrystallized into the epidote-amphibolite assemblage; hornblende + clinozoisite + kyanite + paragonite ± muscovite + chlorite + albite (An_{0-13}) ± staurolite (up to X_{Mg} = 0.36) ± corundum + rutile ± ilmenite. Kyanite often contains earlier stage plagioclase (An_{26-33}) as tiny inclusions. The Fuko Pass metacumulate is characterized by high Al_2O_3 (18.9 – 25.5 wt.%), high CaO (13.1 – 15.3 wt.%) and low SiO_2 (38.7 – 41.1 wt.%), and bears as much as 66 wt. % normative anorthite and 28 wt. % normative olivine. Its FeO^*/MgO is as high as 2.4, and its protolith may be highly fractionated troctolite or anorthosite. The P-T estimation of the kyanite + clinozoisite + paragonite + albite assemblage indicates pressure of 1.5 – 2.1 GPa and temperature of 700 – 850 °C. This condition is only realized at a deeper part of a subduction zone. The breakdown of the kyanite + clinozoisite assemblage into margarite + plagioclase (An_{18-38}) assemblage implies a decompression P-T path passing through the reaction curve: clinozoisite + kyanite + H_2O = margarite + anorthite, which occurs about 1.0 ± 0.1 GPa at 550 ± 50 °C.

The high-pressure and moderate-temperature metamorphism of the Fuko Pass metacumulate is not observed in the gabbroic dikes crosscutting residual peridotite of the Oeyama peridotite body. Although the Fuko Pass metacumulate has been regarded as dismembered cumulate member of a successive sequence of the "Oeyama ophiolite", it should be reinterpreted as an exotic block which may have been trapped somehow by any tectonic process. The high-pressure metamorphism preserved in the Fuko Pass metacumulate may imply the beginning of subduction in the paleo-Pacific margin at Early Paleozoic time.

Key words: kyanite-bearing metabasite, epidote-amphibolite facies, retrograde metamorphism, Fuko Pass metacumulate, Oeyama ophiolite, Early Paleozoic orogeny

Introduction

The troctolitic and anorthositic cumulates are common constituent members of the plagioclase-type ophiolites in orogenic belts (e. g. Ishiwatari, 1985). In some ophiolites, such aluminous cumulates generally suffered ocean-floor metamorphism and hydrothermal alteration in a steep geothermal gradient soon after their formation and before their emplacement. However, similar cumulates which have experienced medium-or high-pressure metamorphism often occur as allochthonous fragments or bodies within the regional metamorphic belts in both continental collision zones and active margins (e. g. Yokoyama, 1980; Kunugiza et al., 1986; Cotkin et al., 1988; Efimov and Potopova, 1992; Tenthorey et al., 1996). The high-pressure and moderate-temperature aluminous metacumulates commonly bear kyanite and rarely staurolite in addition to the common amphibolite-facies mineral assemblage (e. g. Gibson, 1978; 1979; Enami, 1980; Spear, 1982; Selverstone et al., 1984; Ward, 1984; Helms et al., 1987; Yokoyama and Goto, 1987; Gil Ibarguchi et al., 1991; Kuyumjian, 1998). Such a low-variance mineral assemblage and retrograde products of aluminous phases in the metacumulate could allow precise

estimation of P-T path.

The fault-bounded cumulate complex which is now thoroughly recrystallized into epidote-amphibolite facies assemblage including kyanite and staurolite is exposed as the fault-bounded block (or thrust sheet) in the Oeyama peridotite body, easternmost Chugoku Mountains (Kurokawa 1975; Kuroda et al., 1976; Kurokawa, 1985). The metacumulate unit has been regarded as cumulate member of the Oeyama ophiolite, and its metamorphic condition has been estimated to be medium pressure amphibolite-facies (around 0.5 GPa) from the chemistry of hornblende (Kurokawa, 1985). However, the mineral assemblage kyanite + clinozoisite (zoisite) preserved in the metacumulate (Kurokawa, 1985) is stable only in the higher-pressure field greater than around 0.9 GPa (e. g. Storre and Nitsch, 1974; Chatterjee, 1976; Perkins et al., 1980; Jenkins, 1984; Chatterjee et al., 1984), implying metamorphism of at least 25 km depth. In this paper, the author newly defined the epidote-amphibolite as "Fuko Pass metacumulate block", because the metacumulate shows tectono-metamorphic history different from that of the Oeyama ophiolite.

The purposes of this study are (1) to determine the protolith of the Fuko pass metacumulate from the bulk rock composition (major and trace elements), (2) to described petrographic characteristics and to estimate P-T condition and path, and then (3) to discuss tectonic implications of the Fuko Pass metacumulate based on new petrologic data.

Geologic setting

In the Chugoku Mountains of the Inner Zone of southwestern Japan, the 'Oeyama ophiolite' and its equivalents occupy the structurally highest position (Fig. 1) (e. g. Ishiwatari, 1990; Isozaki and Maruyama, 1991; Hayasaka et al., 1995; Tsujimori, 1998; Tsujimori and Itaya, 1999). The Oeyama ophiolite is one of the oldest ophiolites in the circum-Pacific orogenic belt (Ishiwatari, 1994) as old as the Trinity ophiolite of western U. S. A. (Wallin et al., 1988) and an ophiolitic melange of New England Fold Belt in eastern Australia (Aitchison et al., 1992). Although the Oeyama ophiolite does not have complete ophiolitic sequence, it has been generally accepted as an ophiolite nappe, which rests on Late Paleozoic Renge metamorphic belt (including blueschist-bearing serpentinite melange) and the other younger nappes (e.g. Tsujimori and Itaya, 1999). The dismembered ophiolite bodies are composed mainly of moderately depleted harzburgite (residual spinel peridotite) and dunite which are cut by diallage gabbro and dolerite intrusions of MORB-like chemistry. The intrusions commonly occur in peridotite bodies of the Oeyama ophiolite, and recently Hayasaka et al (1995) preliminarily reported Sm-Nd ages of about 560 Ma for the gabbroic intrusions in central Chugoku Mountains, suggesting formation of the Oeyama ophiolite in Cambrian. The Oeyama harzburgite (Kurokawa, 1985; Uda, 1984 identified it as lherzolite) is more fertile than its western counterparts. Podiform chromitites with dunite envelopes are absent in Oeyama, and occur only in the western bodies (Arai, 1980; Matsumoto et al., 1997).

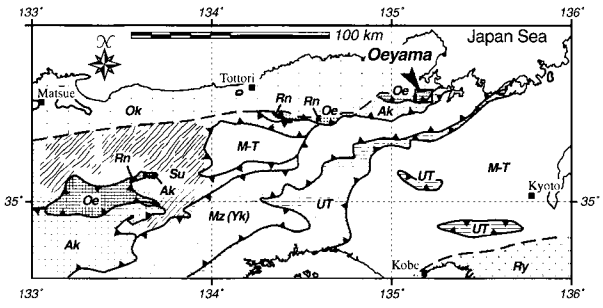

Fig. 1. Simplified distribution map of geotectonic nappe pile in the eastern Chugoku Mountains. Ok : Oki low-P/T metamorphic belt ; Oe : Oeyama ophiolite ; Rn : Renge high-P/T metamorphic belt ; Ak : Akiyoshi accretionary complex ; Mz (Yk) : Mizuru belt (Yakuno ophiolite) ; UT : Ultra-Tamba accretionary complex ; Su : Suo high-P/T metamorphic belt ; M-T : Mino-Tamba accretionary complex ; Ry : Ryoke low-P/T metamorphic belt.

A simplified geologic map of the Oeyama area is shown in Fig. 2. The Oeyama peridotite body (10 km by 3 km in size) may tectonically overlie the Permian accretionary complex on the south (Shimomidami Formation, possibly belonging to Akiyoshi accretionary complex: Ishiga and Suzuki, 1988). The Oeyama peridotite body is mostly composed of massive lherzolitic harzburgite (residual peridotite), which is cut by gabbroic intrusions (diallage gabbro and dolerite) (Uda, 1984; Kurokawa, 1985). The Fuko Pass metacumulate (4.5 km by 1.5 km in size) is exposed only around the topographically highest point of the peridotite body. It gave the hornblende K-Ar ages of 426 and 413 Ma (Nishina et al., 1990).

Both of Fuko Pass metacumulate and Oeyama peridotite were overprinted by contact metamorphism of the Cretaceous granitic intrusions on the north. Uda (1984) divided the contact aureole into five metamorphic zones: Zone I (antigorite), Zone II (olivine + antigorite + diopside), Zone III (olivine + antigorite + tremolite), Zone IV (olivine + talc ± tremolite ± magnesio cummingtonite + tremolite) and Zone V (olivine + enstatite ± tremolite ± hornblende) as approaching the granite. Fuko Pass area belongs to his zone II, but effect of the contact metamorphism is exceptionally scarce in the sampled outcrop.

Sample description and petrography

An outcrop (25 × 5 m) near Fuko Pass described in detail by Kurokawa (1985) is a rare place where one can sample the freshest mafic metacumulate, although considerably weathered in fact. The outcrop is located in the contact aureole (Uda (1984)'s zone II) (Fig. 2), but there is almost no overprinting of contact metamorphism. In this outcrop, the

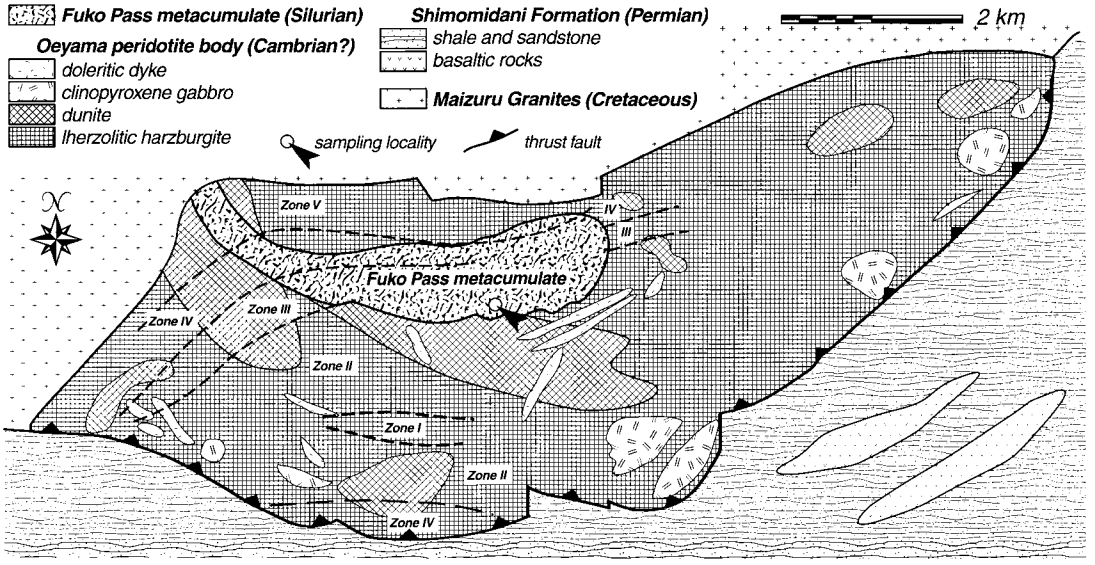

Fig. 2. Geologic map of the Oeyama area. Lithologic distribution and classification of residual peridotite is based on Uda (1984). Distribution of the Fuko Pass metacumulate and other rocks is based on Kurokawa (1985). Broken lines represent the boundary between Uda (1984)'s metamorphic zones of the contact aureole.

relict massive coarse-grained rocks (metamorphosed clinopyroxenite and metagabbro), virtually undeformed, occur as irregular blocks in the matrix of foliated epidote-amphibolite.

The collected samples are divided into foliated epidote-amphibolite and undeformed metagabbro on the basis of the presence or absence of foliation. The latter is subdivided into leucocratic and melanocratic ones by abundance of clinozoisite. They are characterized by a mineral assemblage hornblende + clinozoisite (± zoisite) + kyanite + paragonite (± muscovite) + chlorite + albite (An_{0-13}) ± staurolite ± corundum with rutile and ilmenite as accessories. Kyanite often contains earlier stage plagioclase (An_{26-33}). In addition to this assemblage, retrograde mineral assemblage margarite + paragonite + chlorite ± plagioclase (An_{18-38}) is recognized. Recently, spinel pseudomorphs consisting of corundum-magnetite-gahnite symplectite and relict aluminous clinopyroxene has been found in melanocratic metagabbro ("spinel" metagabbro) (Tsujimori and Ishiwatari, 1998). The texture and modal composition are variable from sample to sample.

1. Foliated epidote-amphibolite

The epidote-amphibolite is moderately foliated, heterogeneous rock. It is commonly medium-grained (1 – 3 mm), but coarse-grained hornblende (up to 5 mm) is also frequent. Hornblende, clinozoisite and kyanite are major constituent minerals, and they form foliation (Fig. 3a). Kyanite often contains plagioclase (An_{26-33}) as tiny inclusion (< 0.03 mm) (Fig. 3b). Paragonite, chlorite, staurolite, albite and rarely muscovite occur as small inclusions in clinozoisite (Fig. 3c). Clinozoisite is optically heterogeneous even in one grain, and zoisite sometimes coexists with clinozoisite. Rutile, ilmenite and sulfide appear as accessories. Ilmenite occurs as both rim and exsolution blebs in rutile. In some cases, large mineral aggregates (up to 5 mm) consisting mainly of staurolite (< 0.5 mm) with minor corundum (< 0.1 mm), chlorite and magnetite are observed. Corundum and magnetite are found only in the aggregates, and kyanite is often observed in the margin of the aggregates. Staurolite of the aggregates is in textural equilibrium with clinozoisite, kyanite, chlorite and corundum (Fig. 3d).

Retrograde minerals occur replacing earlier phases. Margarite often occurs as fibrous coronas replacing kyanite, and paragonite and muscovite are also rarely found in the coronas. Chlorite and tiny plagioclase (An_{18-38}) (< 0.05 mm) are rarely observed as retrograde minerals with margarite replacing kyanite. Kyanite is strongly altered when in contact with clinozoisite, but well-preserved when in contact with hornblende. Secondary chlorite sometimes replaces hornblende.

2. Leucocratic metagabbro

The leucocratic metagabbro is coarse-grained (5 – 15 mm), undeformed rock. It consists mainly of clinozoisite and subordinate amount of hornblende with rutile and magnetite as accessories. Clinozoisite usually contains kyanite, paragonite, chlorite, staurolite and rarely albite as inclusions (Fig. 3e). Kyanite and staurolite occur as euhedral crystal (0.5 – 2.0 mm) in the clinozoisite-rich domain, and they are often mantled by retrograde margarite and paragonite (Fig. 3f). Staurolite rarely includes paragonite. Retrogression in this rock is more obvious than in the foliated epidote-amphibolite.

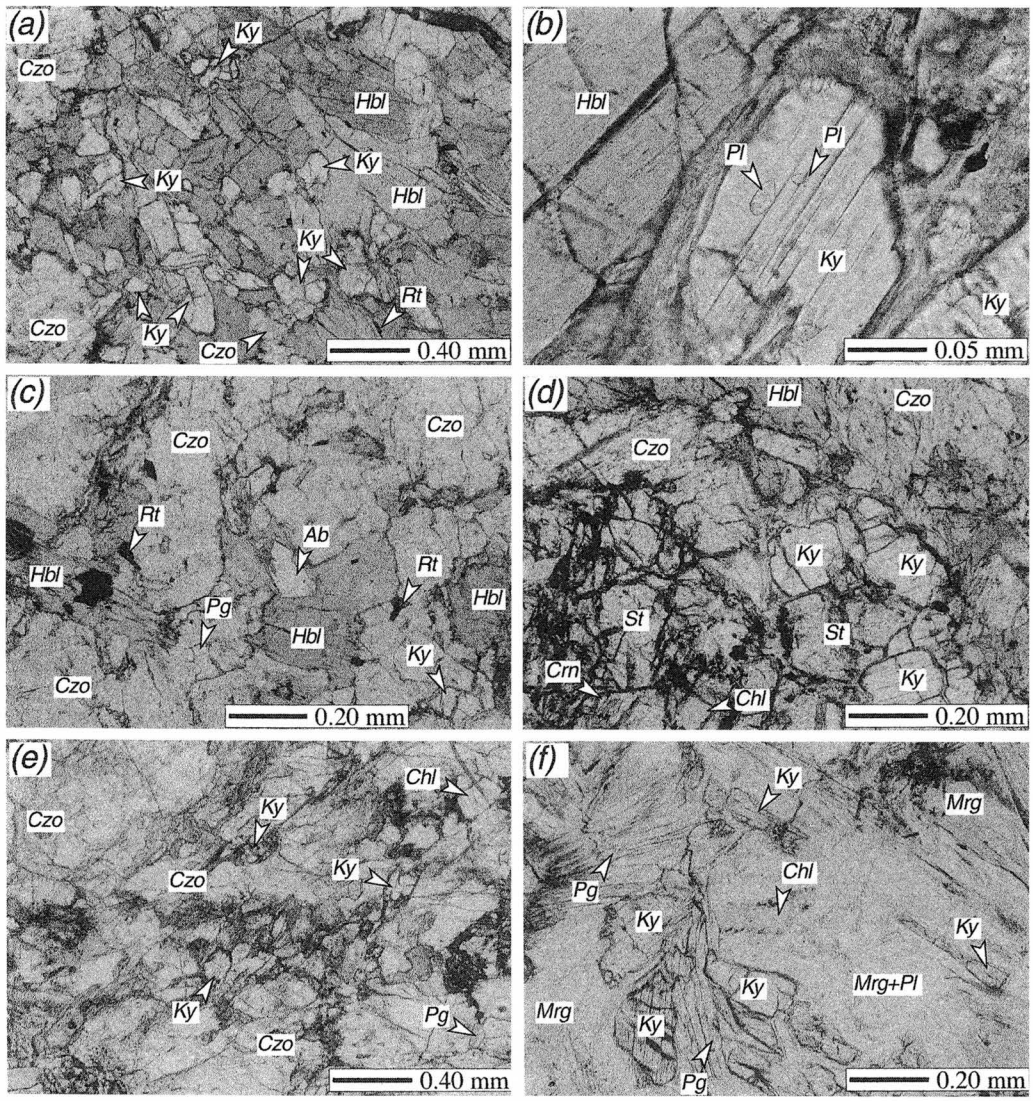

Fig. 3. Photomicrographs of the Fuko Pass metacumulates. (a) Hornblende and kyanite in the foliated epidote-amphibolite. (b) Kyanite with plagioclase inclusions in the foliated epidote-amphibolite. (c) Albite, kyanite and paragonite associated within clinozoisite in the foliated epidote-amphibolite. (d) Staurolite aggregates coexisting kyanite in the foliated epidote-amphibolite. Fine-grained corundum is associated within staurolite. (e) Clinozoisite with kyanite inclusions in the leucocratic metagabbro. (f) Kyanite mostly replaced by margarite aggregates in the leucocratic metagabbro.

3. "Spinel" metagabbro

The "spinel" metagabbro is melanocratic, coarse-grained (5 – 15 mm), undeformed rock. It consists mainly of hornblende, relict aluminous clinopyroxene (up to 8.3 wt.% Al_2O_3), spinel pseudomorph (corundum-magnetite-gahnite symplectite), clinozoisite-zoisite and chlorite, with small amount of kyanite, magnetite, and secondary margarite. This indicates that the Fuko Pass metacumulate has experienced the granulite facies metamorphism prior to the high-pressure metamorphism characterized by kyanite + clinozoisite assemblage. More detailed petrology of the "spinel" metagabbro will be described elsewhere.

Whole-rock chemistry

The major (Si, Ti, Al, Fe, Mn, Mg, Ca, Na, K and P) and trace (Ni, Cu, Zn, Pb, Y and V) elements were analyzed by the Rigaku System 3270 X-ray fluorescence spectrometer with Rh tube at Kanazawa University. The analyses were done at 50 kV accelerating voltage and 20 mA beam current. The other trace elements (Sc, Cr, Co, La, Sm, Eu, Lu and Th) were determined by instrumental neutron activation analysis (INNA method). The INNA samples were activated at the Kyoto University Reactor, and their gamma-ray spectroscopic analyses were done at the Radioisotope Laboratory of Kanazawa University. The result is given in Table 1, and plotted in CaO-MgO, Sr-Ni, and Al_2O_3-FeO*/MgO diagrams (Fig. 4). Whole-rock major element compositions of leucocratic metagabbro, foliated epidote-amphibolite (including Kurokawa (1985)'s data) and "spinel" metagabbro are characterized by high Al_2O_3 (18.9 – 25.5 wt.%), high CaO (13.1 – 15.3 wt.%), low SiO_2 (38.7 – 41.1 wt.%) and low

Table 1. Whole-rock composition of the Fuko Pass metacumulate. Major element composition of epidote-amphibolite described by Kurokawa (1985) is also listed.

	epidote-amphibolite		*leucocratic metagabbro*		*"spinel" metagabbro*	
sample	*EAO1*	*Kurokawa (1985)*	*LCMG01*	*LCMG02*	*SPMG01*	*SPMG02*
Major element concentrations (in weight %)						
SiO_2	41.08	38.70	39.51	39.37	38.86	39.04
TiO_2	0.78	0.78	0.50	0.65	0.56	0.52
Al_2O_3	20.63	23.22	25.46	23.97	19.41	18.92
Fe_2O_3*	12.78	12.85	10.44	11.02	12.31	11.75
MnO	0.16	0.15	0.11	0.12	0.10	0.10
MgO	6.74	6.48	4.38	5.03	11.37	11.19
CaO	14.08	13.46	15.29	15.22	13.09	14.28
Na_2O	1.84	1.42	0.91	1.00	0.88	0.82
K_2O	0.36	0.35	0.58	0.47	0.14	0.11
P_2O_5	0.05	-	0.01	0.01	0.01	0.01
Total	98.50	97.41	97.19	96.86	96.73	96.74
FeO/MgO*	*1.71*	*1.78*	*2.14*	*1.97*	*0.97*	*0.94*
Mg#	*0.45*	*0.47*	*0.51*	*0.50*	*0.65*	*0.65*
Normative compositions (Fe^{3+}/total Fe = 0.2)						
or	2.18	0.00	0.00	0.00	0.00	0.00
ab	0.84	0.00	0.00	0.00	0.00	0.00
an	48.18	58.05	66.08	62.02	50.76	49.71
lc	0.00	1.68	2.79	2.27	0.68	0.53
ne	8.20	6.75	4.33	4.78	4.21	3.92
di	19.02	6.86	6.30	9.33	9.76	11.01
ol	16.13	20.35	14.80	15.33	28.20	26.95
cs	0.00	0.90	1.54	1.64	1.52	3.27
mt	3.80	3.87	3.14	3.33	3.73	3.56
il	1.52	1.54	0.99	1.29	1.11	1.03
ap	0.12	-	0.02	0.02	0.02	0.02
Total	100.00	100.00	100.00	100.00	100.00	100.00
Trace-element compositions (in ppm)						
Sc	43.3	-	30.1	34.5	143.1	135.5
V	536	-	415	425	633	610
Cr	32.5	-	59.2	75.5	64.0	52.3
Co	60.7	-	48.4	40.1	74.4	77.5
Ni	18	-	14	18	97	99
Cu	123	-	273	252	109	105
Zn	92	-	62	71	224	166
Rb	6	-	16	10	n.d.	n.d.
Sr	402	-	479	411	147	139
Y	20	-	10	12	12	11
Zr	25	-	15	15	21	22
Ba	156	-	192	157	144	117
La	1.5	-	n.d.	0.8	0.9	1.2
Sm	2.2	-	1.1	1.3	1.3	1.3
Eu	0.9	-	0.5	0.6	0.5	0.6
Lu	0.3	-	0.1	n.d.	0.2	n.d.
Th	1	-	3	n.d.	4	n.d.

Mg#:Mg/(Mg+Fe^{2+}) atomic ratio

TiO_2 (0.5 – 0.8 wt.%) and $Na_2O + K_2O$ (less than 2.2 wt.%). The bulk rock composition and the calculated normative composition suggest their troctolitic protolith with abundant anorthite-rich plagioclase.

Mineralogy

Chemical analyses of minerals were carried out with a JEOL electron-probe microanalyzer JXA-8800R (wavelength-diversive system) at Kanazawa University, and a JEOL JXA-8900R (wavelength-diversive system) at Okayama University of Science. The analyses were done at 15 kV accelerating voltage, 12 nA probe current on Faraday cup with PCD (probe current detector) and 3 – 5 micrometer probe diameter. Natural and synthetic silicates and oxides are used as standards at both Kanazawa University and Okayama University of Sciences (Tsujimori et al., 1997). The ZAF method was employed for matrix corrections. Ca, Na, K and Al X-ray mapping of retrograde white micas was carried out with a JXA-8800R at 20 kV accelerating voltage and 30 nA probe current. Selected analyses of representative rock-forming minerals are presented in Table 2.

1. Hornblende

The structural formula of hornblende has been calculated using PROBE-AMPH program (Tindle and Webb, 1994) that the estimation of Fe^{2+} and Fe^{3+} for calcic amphibole is based on 13 cations (O = 23) excluding Ca, Na and K. The nomenclature of amphibole is based on the classification by Leake (1978).

Amphiboles of the Fuko Pass metacumulate are mostly tschermakitic hornblende and pargasite, excepting thoese in "spinel" metagabbro (Fig. 5a). They are characterized by high Al_2O_3 content up to 18.0 wt.%. The amphibole of foliated epidote-amphibolite contains 0.62 – 1.16 Al^{VI}, 6.23 – 6.72 Si, 0.26 – 0.49 Na_B and 0.11 – 0.61 $(Na + K)_A$, and that of leucocratic metagabbro bears 0.40 – 1.03 Al^{VI}, 6.23 – 6.56 Si, 0.29 – 0.31 Na_B and 0.15 – 0.70 $(Na + K)_A$. The compositional trend of amphiboles in the Fuko Pass metacumulate is plotted on the Dalradian field of Laird and Albee (1981)'s Al^{IV} versus $Al^{VI} + Fe^{3+} + Ti$ diagram (Fig. 5b), and it roughly corresponds to that of the other Al-rich metabasites in medium-to high-pressure metamorphic belts. $Mg/(Mg + Fe^{2+})$ ratio is 0.59 – 0.79 for the foliated epidote-amphibolite and 0.61 – 0.78 for the leucocratic metagabbro, and is significantly lower than that of "spinel" metagabbro (0.78 – 0.92). Although Na_B, Ti and $Na/(Ca + Na)$ ratio are roughly constant for $Fe^{2+}/(Fe^{2+} + Mg)$ ratio and Si, $Fe^{3+}/(Al^{VI} + Fe^{3+} + Ti)$ ratio has linear negative correlation with $Fe^{2+}/(Fe^{2+} + Mg)$ ratio.

2. Staurolite

The structural formula of staurolite has been calculated on the basis of O = 46 as Li_2O and H_2O-free. Staurolite of the Fuko Pass metacumulate shows wide variation of the $Mg/(Mg + Fe)$ ratio ranging from 0.16 to 0.36, and it contains significant ZnO (up to 2 wt.%) in solid solution. The composition has a good negative correlation of $Fe + Mg + Zn$ against $Si + Al^{VI} + Ti$. The correlation overlaps a structural formula, $(Mg + Fe)_{3+1.5x}Al_{18-x}Si_8O_{46}$, which represents Mg-rich staurolites in the corundum-bearing epidote-amphibolite of the Sambagawa metamorphic belt (Yokoyama and Goto, 1988). The MgO and $Mg/(Mg + Fe)$ ratio of the foliated epidote-amphibolite is higher than those of the leucocratic metagabbro (Fig. 6a). However, staurolite is richer in ZnO in the leucocratic metagabbro than in the foliated epidote-amphibolite (Fig. 6b). The difference of Mg content in staurolite corresponds to the different whole-rock composition, but Zn content is inconsistent with that (Table 1). Affinity of staurolite for zinc is well known among both metapelites and metabasites (e.g. Goodman, 1993; Sato and Azanon, 1993). Zn content of staurolite of the Fuko Pass metacumulate is higher

Table 2. Selected microprobe analysis of the rock-forming minerals. (a) foliated metagabbro; (b) leucocratic metagabbro.

(a)	*hornblende*		*staurolite*		*clinozoisite & zoisite*			*white micas*					*plagioclase*			*chlorite*	*kyanite*	*corundum*
wt.%					*Czo*	*Czo*	*Zo*	*Pg [Czo]*	*Ms [Czo]*	*Pa [St]*	*Ma (retro)*	*Ms (retro)*	*Pl [Ky]*	*Ab [Czo]*	*Pl (retro)*			
SiO_2	40.23	42.21	28.89	28.86	39.27	38.57	39.29	44.74	46.42	40.43	30.29	46.74	59.83	68.06	62.62	27.56	37.32	0.00
TiO_2	0.66	0.38	0.27	0.26	0.00	0.00	0.01	0.09	0.95	0.07	0.24	0.04	0.00	0.04	0.05	0.15	0.13	0.01
Al_2O_3	17.97	17.05	52.25	52.98	28.83	27.22	31.50	39.69	34.38	42.31	49.71	36.28	25.06	19.74	23.23	22.28	61.38	98.79
Cr_2O_3	0.00	0.01	0.00	0.00	0.00	0.00	0.00	0.00	0.06	0.00	0.00	0.05	0.01	0.00	0.01	0.05	0.04	0.04
Fe_2O_3*	-	-	-	-	6.56	8.99	3.06	-	-	-	-	-	0.17	0.44	0.27	-	1.17	1.21
FeO**	14.87	13.824	11.64	11.39	-	-	-	0.69	1.81	0.75	0.70	0.46	-	-	-	13.61	-	-
MnO	0.24	0.15	0.48	0.54	0.11	0.28	0.05	0.06	0.08	0.00	0.00	0.03	0.01	0.09	0.01	0.19	0.06	0.03
MgO	9.24	9.77	3.03	2.91	0.11	0.15	0.01	0.11	1.02	0.22	0.47	0.06	0.00	0.00	0.00	23.08	0.02	0.02
CaO	10.66	10.38	0.01	0.02	22.87	22.56	24.05	1.88	0.18	5.15	11.64	0.28	6.41	0.61	4.32	0.37	0.19	0.06
Na_2O	3.22	2.92	-	-	0.01	0.00	0.00	6.94	1.82	5.05	1.27	0.12	8.36	11.44	9.79	0.00	0.00	0.01
K_2O	0.06	0.16	-	-	0.00	0.00	0.01	0.00	8.60	0.01	0.00	11.25	0.01	0.02	0.00	0.06	0.02	0.00
ZnO	-	-	0.82	0.67	-	-	-	-	-	-	-	-	-	-	-	-	-	-
Total	97.16	96.84	96.57	96.96	97.76	97.76	97.98	94.18	95.32	94.00	94.30	95.30	99.87	100.44	100.29	87.35	100.33	100.18
atomic ratio																		
O=	*23*	*23*	*46*	*46*	*25*	*25*	*25*	*22*	*22*	*22*	*22*	*22*	*8*	*8*	*8*	*28*	*5*	*3*
Si	5.921	6.176	8.014	7.968	6.073	6.025	6.005	5.814	6.165	5.322	4.193	6.201	2.672	2.969	2.771	5.466	1.006	0.000
Ti	0.074	0.042	0.056	0.054	0.000	0.000	0.001	0.009	0.095	0.007	0.014	0.004	0.000	0.001	0.001	0.022	0.001	0.000
Al	3.118	2.940	17.082	17.240	5.254	5.012	5.674	6.078	5.381	6.563	7.740	5.672	1.319	1.015	1.211	5.208	1.962	1.982
Cr	0.000	0.001	0.000	0.000	0.000	0.000	0.000	0.000	0.006	0.000	0.006	0.005	0.000	0.000	0.000	0.008	0.001	0.000
Fe^{3+}	0.601	0.512	-	-	0.764	1.056	0.352	-	-	-	-	-	0.006	0.015	0.009	-	0.018	0.016
Fe^{2+}	1.229	1.180	2.700	2.630	-	-	-	0.075	0.201	0.083	0.086	0.051	-	-	-	2.257	-	-
Mn	0.030	0.019	0.113	0.126	0.015	0.037	0.006	0.006	0.009	0.000	0.000	0.003	0.000	0.003	0.000	0.032	0.000	0.000
Mg	2.028	2.132	1.253	1.198	0.024	0.034	0.002	0.021	0.202	0.042	0.095	0.013	0.000	0.000	0.000	6.824	0.007	0.000
Ca	1.681	1.627	0.003	0.006	3.788	3.777	3.938	0.261	0.026	0.727	1.578	0.040	0.307	0.029	0.205	0.079	0.006	0.001
Na	0.920	0.829	0.000	0.000	0.003	0.000	0.000	1.747	0.469	1.290	0.413	0.031	0.724	0.967	0.840	0.000	0.000	0.000
K	0.011	0.030	0.000	0.000	0.001	0.000	0.002	0.000	1.457	0.002	0.004	1.904	0.001	0.001	0.000	0.015	0.001	0.000
ZnO	-	-	0.168	0.137	-	-	-	-	-	-	-	-	-	-	-	-	-	-
Total	15.612	15.485	29.221	29.221	15.920	15.941	15.981	14.012	14.010	14.035	14.128	13.924	5.028	5.000	5.038	19.911	3.003	2.001

*: Total Fe as Fe_2O_3. (retro): retrograde products.
**: Total Fe as FeO. [*i*]: inclusions within mineral *i*.

(b)	*hornblende*		*staurolite*		*clinozoisite & zoisite*			*white micas*				*plagioclase*		*chlorite*	*kyanite*
wt.%					*Czo*	*Czo*	*Zo*	*Pg [Czo]*	*Ma (retro)*	*Pg (retro)*	*Ms (retro)*	*Ab [Czo]*	*Pl (retro)*		
SiO_2	44.02	44.74	28.67	28.67	39.22	39.07	39.62	46.08	30.94	45.80	45.12	68.64	58.38	26.45	37.58
TiO_2	0.70	0.73	0.26	0.51	0.03	0.09	0.01	0.12	0.01	0.04	0.33	0.00	0.09	0.03	0.00
Al_2O_3	14.28	12.57	53.17	53.05	29.14	27.79	31.80	37.95	49.68	40.60	35.27	19.42	25.87	23.13	61.78
Cr_2O_3	0.02	0.01	0.01	0.06	0.00	0.01	0.00	0.00	0.00	0.02	0.09	0.03	0.12	0.00	0.00
Fe_2O_3*	-	-	-	-	5.61	8.35	2.64	-	-	-	-	0.32	0.93	-	1.11
FeO**	14.21	14.15	11.44	11.03	-	-	-	0.60	0.49	0.49	0.87	-	-	17.73	-
MnO	0.14	0.23	0.36	0.31	0.07	0.04	0.02	0.00	0.03	0.01	0.08	0.00	0.12	0.06	0.00
MgO	11.10	11.88	1.76	1.98	0.06	0.08	0.00	0.07	0.35	0.07	0.56	0.00	0.00	19.62	0.00
CaO	10.65	10.43	0.08	0.07	23.47	22.20	24.14	0.86	12.49	0.80	0.05	0.46	7.83	0.11	0.02
Na_2O	2.67	2.85	-	-	0.02	0.04	0.00	7.13	0.85	7.21	0.52	11.50	7.07	0.01	0.00
K_2O	0.25	0.24	-	-	0.00	0.00	0.00	0.45	0.00	0.54	10.61	0.01	0.05	0.01	0.02
ZnO	-	-	1.53	1.49	-	-	-	-	-	-	-	-	-	-	-
Total	98.03	97.83	95.75	95.68	97.61	97.66	98.23	93.26	94.83	95.58	93.50	100.38	100.46	87.13	100.51
atomic ratio															
O=	*23*	*23*	*46*	*46*	*25*	*25*	*25*	*22*	*22*	*22*	*22*	*8*	*8*	*28*	*5*
Si	6.363	6.473	7.971	7.965	6.066	6.074	6.027	6.029	4.128	5.852	6.122	2.986	2.606	5.363	1.012
Ti	0.076	0.080	0.054	0.107	0.003	0.010	0.001	0.011	0.001	0.004	0.034	0.000	0.003	0.004	0.000
Al	2.432	2.144	17.423	17.370	5.312	5.092	5.702	5.852	7.813	6.114	5.640	1.001	1.361	5.527	1.961
Cr	0.003	0.001	0.002	0.013	0.000	0.001	0.000	0.000	0.000	0.002	0.010	0.001	0.004	0.000	0.000
Fe^{3+}	0.643	0.673	-	-	0.653	0.977	0.302	-	-	-	-	0.010	0.031	-	0.023
Fe^{2+}	1.074	1.039	2.660	2.563	-	-	-	0.066	0.055	0.052	0.099	-	-	3.008	-
Mn	0.017	0.028	0.085	0.073	0.009	0.005	0.003	0.000	0.003	0.001	0.009	0.000	0.005	0.010	0.000
Mg	2.393	2.562	0.729	0.820	0.013	0.018	0.000	0.013	0.069	0.013	0.113	0.000	0.000	5.931	0.000
Ca	1.649	1.616	0.024	0.021	3.890	3.698	3.935	0.121	1.786	0.110	0.007	0.021	0.375	0.023	0.001
Na	0.747	0.798	0.000	0.000	0.006	0.011	0.000	1.807	0.220	1.786	0.137	0.978	0.612	0.003	0.000
K	0.000	0.045	0.000	0.000	0.000	0.000	0.000	0.075	0.000	0.087	1.836	0.000	0.003	0.003	0.001
ZnO	-	-	0.314	0.306	-	-	-	-	-	-	-	-	-	-	-
Total	15.396	15.460	28.948	28.931	15.952	15.886	15.970	13.975	14.075	14.022	14.006	4.997	5.000	19.872	2.997

*: Total Fe as Fe_2O_3. (retro): retrograde products.
**: Total Fe as FeO. [*i*]: inclusions within mineral *i*.

than the other metabasites (Fig. 6b). One staurolite grain in the foliated epidote-amphibolite contains up to 1.1 wt.% MnO.

In the last decade, Mg-rich staurolite has been treated as a critical mineral of the high to ultra-high pressure metamorphic rocks (e.g. Chopin, 1987; Schreyer, 1988). The Mg-staurolite component in the staurolite solid solution seems to be a function of the metamorphic pressure (Fig. 6a). However, the Mg-rich staurolite-bearing rocks generally have extremely high-Mg whole rock chemistry (e.g. Schreyer et al., 1984; Enami and Zhang, 1988; Gil Ibarguchi et al., 1991). The other constituent minerals also have high Mg/(Mg + Fe) ratio consistent with the high-Mg whole-rock chemistry (e.g. Ward, 1984; Yokoyama and Goto, 1987). It is natural to think that the composition of staurolite not only depends on pressure but also on whole-rock chemistry.

3. Clinozoisite and zoisite

Clinozoisite in the Fuko Pass metacumulate mostly has a moderate pistacite molecule (10 – 24 mole %) (Fig. 7). Zoisite contains 3 – 7 % pistacite molecule, and it coexists with heterogeneous clinozoisite with moderate pistacite molecule. The clinozoisite with considerably higher pistacite component (26 – 29 mole %) is rarely found in the foliated epidote-amphibolite and "spinel" metagabbro.

Naturally coexisting zoisite-clinozoisite pairs were examined by Enami and Banno (1980), and the relationship between their compositions and temperature was experimentally determined by Prunier and Hewitt (1985). In the Fuko Pass metacumulate, compositions of the coexisting zoisite and clinozoisite pairs suggest approximate temperatures up to 600°C.

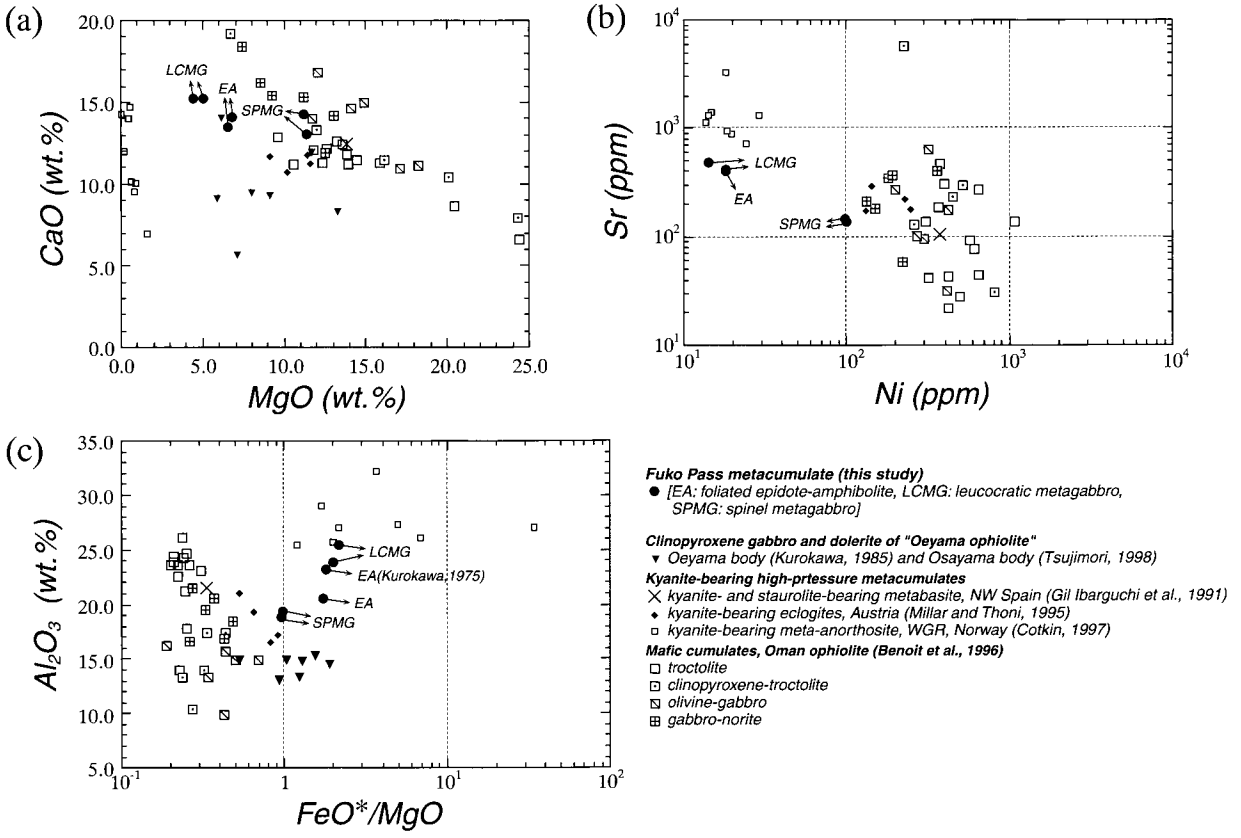

Fig. 4. (a) CaO versus MgO (wt.%), (b) FeO*/MgO versus Al_2O_3 (wt.%) and (c) Ni (ppm) versus Sr (ppm) diagrams showing chemical characteristics of the Fuko Pass metacumulate. The compositions of cumulate rocks of the Oman ophiolite and the other kyanite-bearing metabasites are also plotted for comparison.

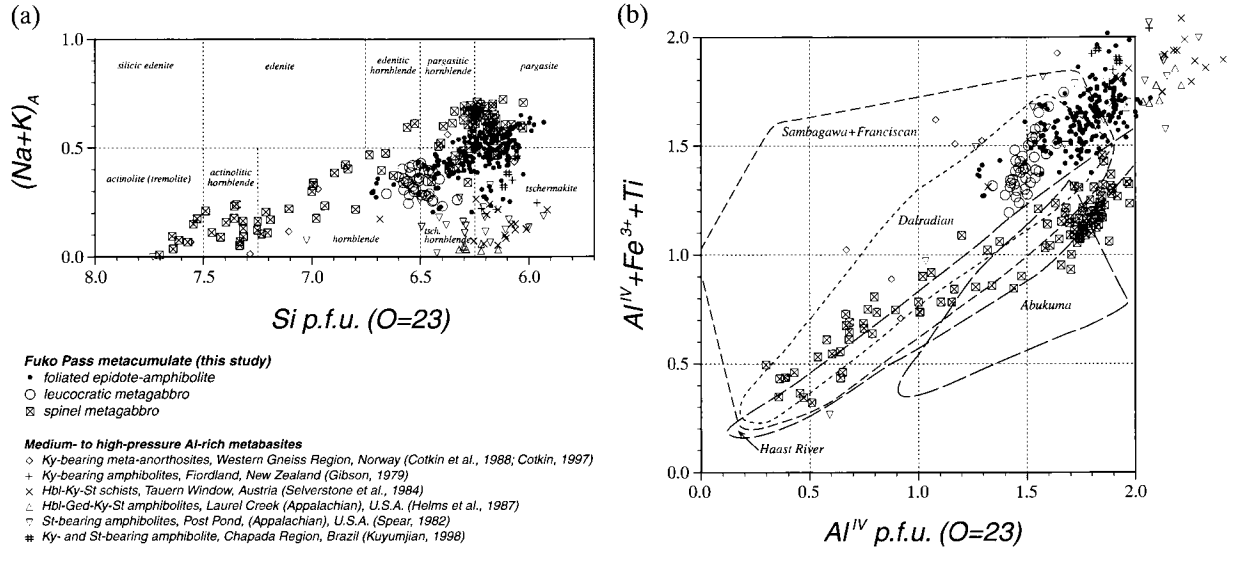

Fig. 5. Chemical composition of amphiboles. (a) Si versus $(Na+K)_A$ diagram. (b) Laird and Albee (1981)'s Al^{IV} versus $Al^{VI}+Fe^{3+}+Ti$ diagram for amphiboles. The amphibole compositions from the other kyanite-bearing metabasites are also plotted.

4. White micas (margarite-paragonite-muscovite)

Paragonite and muscovite of early stage occur as inclusions within clinozoisite and staurolite (only paragonite), suggesting that they were in equilibrium with the host minerals or crystallized earlier than the host. On the other hand, retrograde margarite occurs replacing of kyanite, and it often coexists with retrograde paragonite and muscovite. Chemical compositions of white micas are shown in the paragonite (Na) - muscovite (K) -margarite (Ca) ternary diagrams (Fig. 8). The paragonite inclusion has composition of $Pg_{75-92}Mrg_{8-20}Ms_{<11}$ in

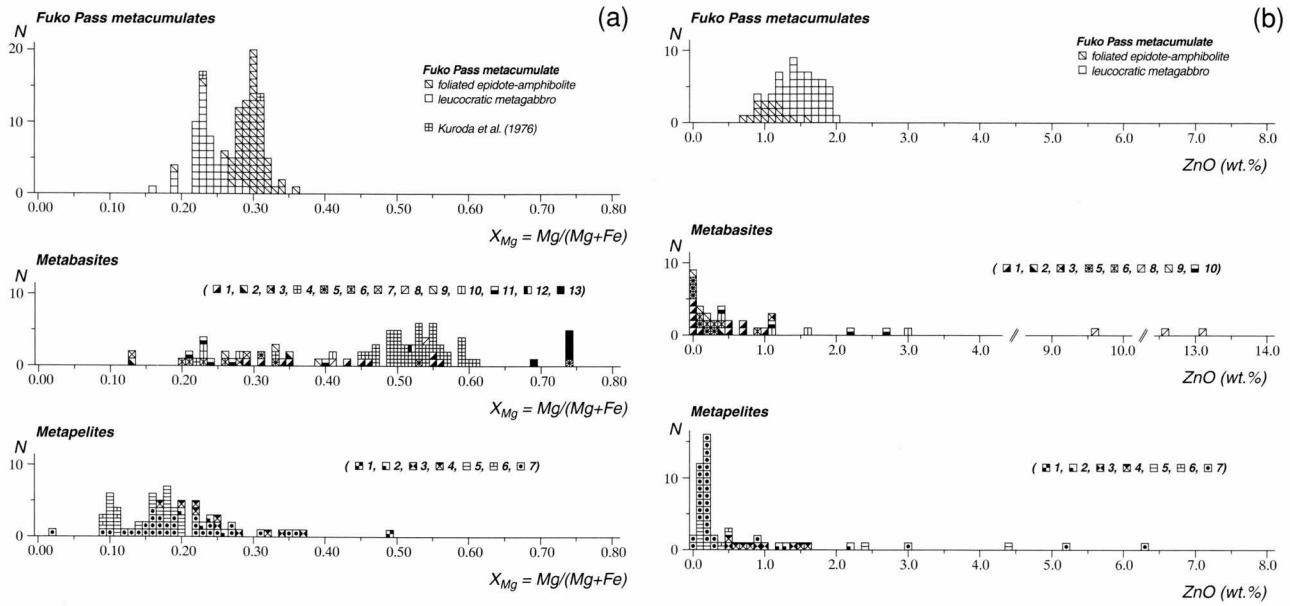

Fig. 6. Frequency distribution of (a) the values of Mg/(Mg+Fe) ratio and (b) ZnO content (wt.%) for staurolite. The staurolite compositions from the other metabasites are also plotted. Metabasites [1: metatroctolite, Fiordland, New Zealand (Ward, 1984); 2: amphibolite, Fiordland, New Zealand (Gibson, 1978); 3: Ky-St amphibolite, Chapadaregion, central Brazil (Kuyumjian, 1998), 4: eclogitic epidote-amphibolite, Sambagawa metamorphic belt, SW Japan (Yokoyama and Goto, 1987); 5: meta-ultrabasic rock and eclogite, Cabo Ortegal, NW Spain (Gil Ibarguchi et al., 1991); 6: Hbl-Ky-St schist, Tauern Window, Austria (Selverstone et al., 1984); 7: amphibolite, Vinjamura, South India (Moeen, 1991); 8: matabasites, Betic Cordillera, SE Spain (Sato and Azanon, 1993); 9: amphibolite, Laurel Creek, Georgia Blue Ridge, U.S. (Helms at al., 1987); 10: Amphibolite, Mt. Cube Quadrangle, Vermont, U.S. (Spear, 1982); 11: Tlc-Phl-Crn-Chl schist, Victoria Land, Antarctica (Grew and Sandiford, 1984); 12: metatroctolites, Vohibory, Madagascar (Nicollet, 1986); 13: Grt-Crn rock and eclogite, Donghai, East China (Enami and Zang, 1988)]. Metapelites [1: Sapphirine-garnet rocks, Limpopo Belt, (Schreyer et al., 1984); 2: Khondalites and pelitic granulite, Sri Lanka (Hiroi et al., 1994); 3: Pelitic gneiss, East Antarctica (Grew et al., 1990); 4: Pelitic gneiss, Hidaka metamorphic belt, Japan (Osanai and Owada, 1990); 5: Pelitic schist, Unazuki metamorphic belt, Japan (Hiroi, 1983); 6: high-Al pelitic schist cobble, Tetori Formation Japan (Tsujimori, 1995); 7: amphibolite-facies metapelites (Holdaway et al., 1986)].

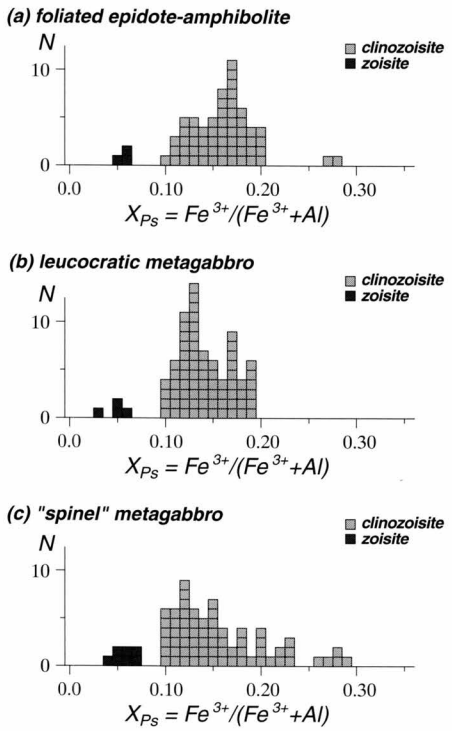

Fig. 7. Frequency distribution of the values of $Fe^{3+}/(Al+Fe^{3+})$ ratio for clinozoisites and zoisites in (a) foliated epidote-amphibolite, (b) leucocratic metagabbro and (c) "spinel" metagabbro.

clinozoisite of the foliated epidote-amphibolite, and $Pg_{76-90}Mrg_{5-15}Ms_{0-13}$ in the leucocratic metagabbro. On the other hand, paragonite inclusion within staurolite is extremely rich in margarite molecule, and has an intermediate composition between paragonite and margarite ($Pg_{52-64}Mrg_{36-47}Ms_{<1}$). In the foliated epidote-amphibolite, muscovite that rarely occurs as inclusion within clinozoisite, has a significantly higher paragonite molecule ($Pg_{17-24}Mrg_{<1}Ms_{75-82}$). X-ray element mapping for Ca, Na, K and Al of retrograde white micas in the leucocratic metagabbro is shown in Fig. 9. Most margarite built up coronitic aggregates around kyanite and staurolite. Paragonite and muscovite partly replace kyanite. This textural relation indicates that association of three white micas postdated kyanite and clinozoisite. Margarite has wide compositional range on the paragonite-margarite join. They have a composition of $Pg_{8-27}Mrg_{73-91}Ms_{<2}$ in the foliated epidote-amphibolite and $Pg_{7-37}Mrg_{61-93}Ms_{<4}$ in the leucocratic metagabbro. Although the retrograde paragonite in the foliated epidote-amphibolite is too fine to be analysed with electron-probe microanalyzer, the retrograde paragonite ($Pg_{77-93}Mrg_{2-19}Ms_{<17}$) in the leucocratic metagabbro has a composition similar to that of inclusion within clinozoisite. Retrograde muscovite is characterized by low paragonite molecule, and its composition

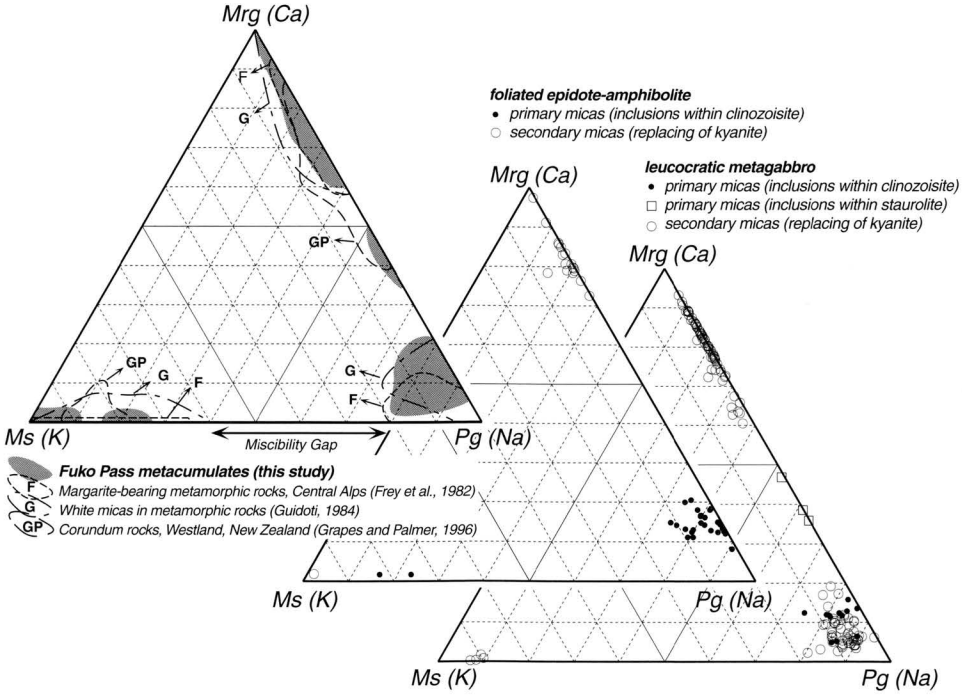

Fig. 8. The paragonite (Na)-muscovite (K)-margarite (Ca) ternary diagrams for white micas. Compositional ranges compiled by Frey et al. (1982) and Guidotti (1984) and the those of corundum-rocks from Westland, New Zealand (Grapes and Palmer, 1996) are also shown.

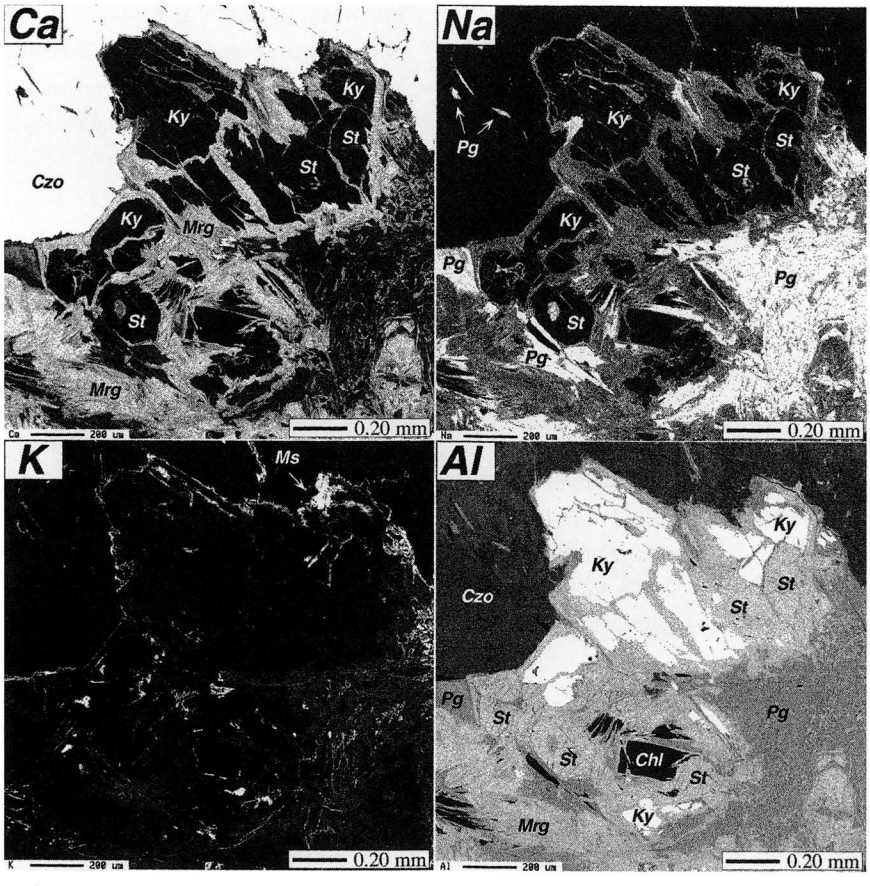

Fig. 9. EPMA X-ray element mapping for Ca, Na, K and Al of retrograde white micas in the leucocratic metagabbro.

is $Pg_2Mrg_2Ms_{96}$ in the foliated epidote-amphibolite and $Pg_{7-10}Mrg_{<2}Ms_{90-93}$ in the leucocratic metagabbro.

The dioctahedral white mica solid solution between paragonite, muscovite and margarite end-members shows wide immiscibility (Fig. 8). The coexisting margarite-paragonite or margarite-muscovite pairs have been reported from some margarite localities (e.g. Ackermand and Morteani, 1973; Enami, 1980; Selverstone et al., 1984; Grapes and Palmer, 1996). The coexisting margarite-paragonite-muscovite three mica assemblage has also rarely been described (e.g. Hock, 1974; Guidotti et al., 1979; Okuyama-Kusunose, 1985; Shiba et al., 1988).

5. Plagioclase

Three different generations of plagioclase are observed in the Fuko Pass metacumulate. Anorthite component in each occurrence is shown in Fig. 10. Albite occurring as inclusion in clinozoisite has 0 – 13 mole % anorthite in solid solution. On the other hand, plagioclase inclusions within kyanite are considerably much more calcic, containing 26 – 33 mole % anorthite. The retrograde plagioclase, which occurs as replacement products of kyanite and coexists with margarite, contains 18 – 38 mole % anorthite.

6. Other minerals

Kyanite contains significant Fe_2O_3 (0.7 – 1.3 wt.%) in solid solution. No chemical difference of kyanite is observed between the foliated epidote-amphibolite and leucocratic metagabbro.

Corundum contains 0.8 – 1.2 wt.% Fe_2O_3. Its Fe_2O_3 content is significantly higher than that of corundum in metabasites from the other localities (mostly less than 0.4 wt.%; e.g. Minakawa and Momoi, 1982; Enami and Zang, 1988; Morishita and Kodera, 1998).

Chlorite in the foliated epidote-amphibolite is richer in Mg/(Mg + Fe) ratio (0.71 – 0.77) than that of the leucocratic metagabbro (0.64 – 0.67), assuming no ferric iron. This suggests the control of whole-rock composition on the chlorite compositions. Chlorites in both foliated epidote-amphibolite and leucocratic metagabbro are characterized by low Si (5.3 – 5.5 p.f.u. for O = 28) and high Al (5.1 – 5.8 p.f.u.), and plotted within the field of ripidolite composition (Hey, 1954). No systematic chemical difference is observed in spite of their texture.

Rutile bears 0.3 – 0.8 wt.% Fe_2O_3.

Ilmenite contains up to 2.0 wt.% MnO.

Discussion

1. Origin of the Fuko Pass metacumulate

Although the Fuko Pass metacumulate block had been thoroughly metamorphosed and variously deformed, the bulk rock composition (major and trace elements) and normative mineralogy constrain cumulus origin. In the Fuko Pass metacumulate here studied, 48 – 66 wt. % normative anorthite and 16 – 28 wt. % normative olivine are calculated. The compositional variability is best illustrated in Fig. 4. The negative correlation between CaO and MgO (Fig. 4a) indicates mixture of anorthitic plagioclase and olivine. This is compatible with a negative correlation between Sr and Ni, which are concentrated in plagioclase and olivine, respectively (Fig. 4b). The leucocratic metagabbro shows more fractionated feature than epidote-amphibolite and "spinel" metagabbro. Al_2O_3 is increasing with FeO^*/MgO (Fig. 4c). It may correspond to modal increase of anorthite-rich plagioclase with fractionation.

The FeO^*/MgO ratio of the Fuko Pass metacumulates (0.9 – 2.1) are considerably higher than the mafic cumulate rocks of the Oman ophiolite (Benoit et al., 1996) and the other kyanite-bearing metabasites of cumulate origin excepting for meta-anorthosite of Western Gneiss Region (Cotkin, 1997). This suggests the high degree of fractionation for magma that produced the protoliths of the Fuko Pass metacumulate.

The troctolitic and anorthositic cumulate occurs commonly in the plagioclase-type ophiolites (i.e. lower portion of oceanic crust) or in large layered plutonic complex such as Bushveld and Stillwater. In the Fuko Pass metacumulate, melanocratic metagabbro ("spinel" metagabbro) preserves granulite-facies minerals prior to epidote-amphibolite facies (Tsujimori and Ishiwatari, 1998). It is possible that the Fuko Pass metacumulate represent a lower part of unusually thick oceanic crust beneath oceanic plateau or oceanic island arc, because the granulite-facies metamorphic condition is realized in the lower part of 15 – 40 km-thick crust.

2. Metamorphic condition

Although any geothermometers based on Fe-Mg exchange reactions are not applicable for the Fuko Pass metacumulate, its approximate P-T condition can be deduced by the mineral assemblage. In the Fuko Pass metacumulate, some important reaction lines, which have been experimentally determined or thermodynamically calculated, constrain their metamorphic P-T condition and path. The thermodynamic calculations in this paper are based on THERMOCALC (ver. 2. 5) program (Powell and Holland, 1988; Holland and Powell, 1990).

High-pressure metamorphic stage

1) Kyanite + paragonite + albite + clinozoisite assemblage

The assemblage kyanite + clinozoisite (zoisite) is stable at the pressure higher than about 0.9 GPa in the pure CASH (CaO-Al_2O_3-SiO_2-H_2O) system (e.g. Storre and Nitsch, 1974; Chatterjee, 1976; Perkins, 1979; Jenkins, 1984; Chatterjee et al., 1984; Halbach and Chatterjee, 1984). The simplified CASH reactions:

clinozoisite + kyanite + H_2O = margarite + quartz (1),

clinozoisite + kyanite = margarite + anorthite (2), and

clinozoisite + kyanite = anorthite + corundum + H_2O (3).

give low-pressure limit for the assemblage clinozoisite +

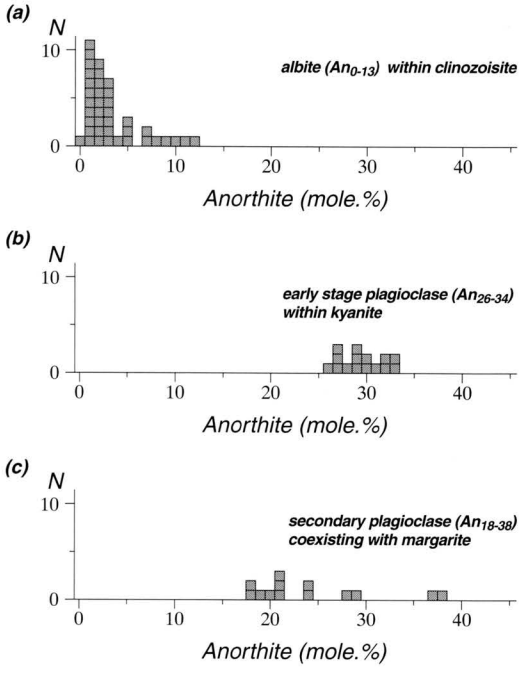

Fig. 10. Frequency distribution of the anorthite component for (a) albite inclusions within clinozoisite, (b) early stage plagioclase inclusions within kyanite and (c) secondary plagioclase coexisting margarite.

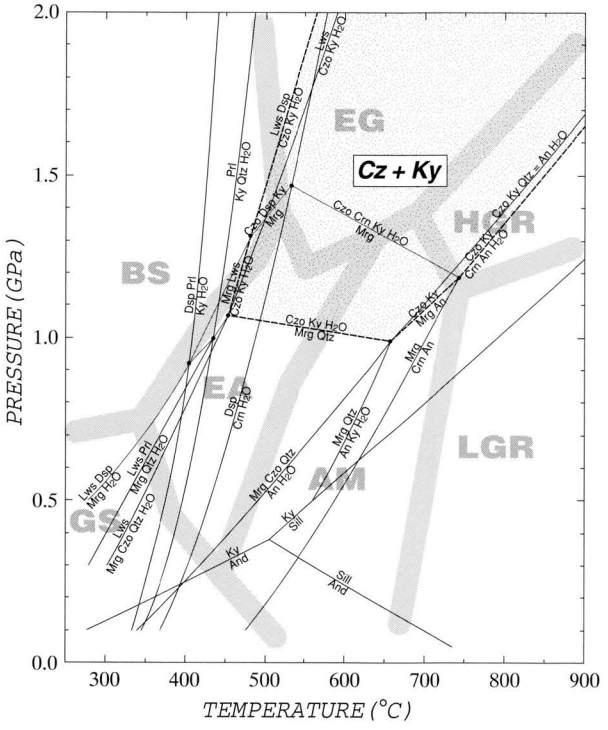

Fig. 11. Phase diagram for the CASH (CaO-Al_2O_3-SiO_2-H_2O) system on pressure-temperature diagram. All the curves were obtained with THERMOCALC (ver. 2.5) program of Holland and Powell (1990). The petrogenetic grid for common basaltic system proposed by Oh and Liou (1998) is also drawn (GS : greenschist facies ; BS : blueschist facies ; EA : epidote-amphibolite facies ; AM : amphibolite facies ; LGR : low-pressure granulite facies ; HGR : high-pressure granulite facies ; EG : eclogite facies). Abbreviations [Ky : kyanite, Czo : clinozoisite, Crn : corundum, Mrg : margarite, Lws : lawsonite, An : anorthite, Dsp : diaspor, Prl : pyrophyllite, Qtz : quartz, Ky : kyanite ; Sill : sillimanite ; And : andalusite].

kyanite in the CASH system (Fig. 11), though the location of the stability field in the P-T space is significantly moved by the effects of solid solution. The stability field is moved to the low pressure side by the increase of pistacite component in clinozoisite and to higher pressure side by the increase of albite component in plagioclase. The presence of earlier stage plagioclase (An_{26-33}) in kyanite gives low-pressure and high-temperature limits for high-pressure stage (Fig. 12).

As mentioned before, clinozoisite contains kyanite, paragonite and albite, which are in textural equilibrium with host clinozoisite. The simplified CASH and NASH (Na_2O-Al_2O_3-SiO_2-H_2O) reactions:

clinozoisite + kyanite = anorthite + corundum + H_2O (3),

paragonite = jadeite + kyanite + H_2O (4), and

paragonite = jadeite + kyanite + H_2O (5).

define pressure-temperature limit for the assemblage kyanite + paragonite + albite + clinozoisite. If the clinozoisite ($a_{Czo} = X_{Al}^{M3} = 0.6$) and plagioclase ($a_{An} = X_{An} = 0.26$), where a_i is activity of the mineral end-member i, are applied for the thermodynamic calculation, the pressure-temperature condition is limited at a P-T space of 1.5 – 2.1 GPa at 700 – 850°C.

2) Kyanite- and staurolite-bearing equilibrium

The Fuko Pass metacumulate includes the unusual mineral assemblage of hornblende + kyanite + staurolite. This assemblage has only been known from some high-pressure and intermediate temperature metabasites (e.g. Fiordland, New Zealand: Gibson, 1978; Tauern Window, Austrian Alps: Selverstone et al., 1984; Blue Ridge, Appalachians: Helms et al., 1987; Iberian massif: Gil Ibarguchi et al., 1991; Chapada, Brazil: Kuyumjian, 1998). Selverstone et al. (1984) and Helms et al. (1987) argued that an assemblage kyanite + staurolite + hornblende reflects pressures higher than those appropriate for the stability of the common amphibolite assemblage. Froese and Hall (1983) presented a Schreinemakers' nets which clearly constrains the natural occurrences of the assemblage kyanite + staurolite to higher pressure condition than the common amphibolite assemblage. Recently, Lattard and Bubenik (1995) experimentally revealed that the complete Fe-Mg solid solution of staurolite is stable at 720 – 800°C at 2 GPa with or without oxygen buffers (WM, NNO, and MH) in the system FMASH (FeO-MgO-Al_2O_3-SiO_2-H_2O). Furthermore, Daniels et al. (1996) found staurolite (Mg/(Mg +Fe) = 0.21) inclusion in a diamond crystal from the Dokolwayo kimberlite, NE Swaziland. This suggests that Mg content of natural staurolite may do not depend on pressure. Schreyer (1988) argued that Mg-staurolite was produced by the low-temperature reaction in the system

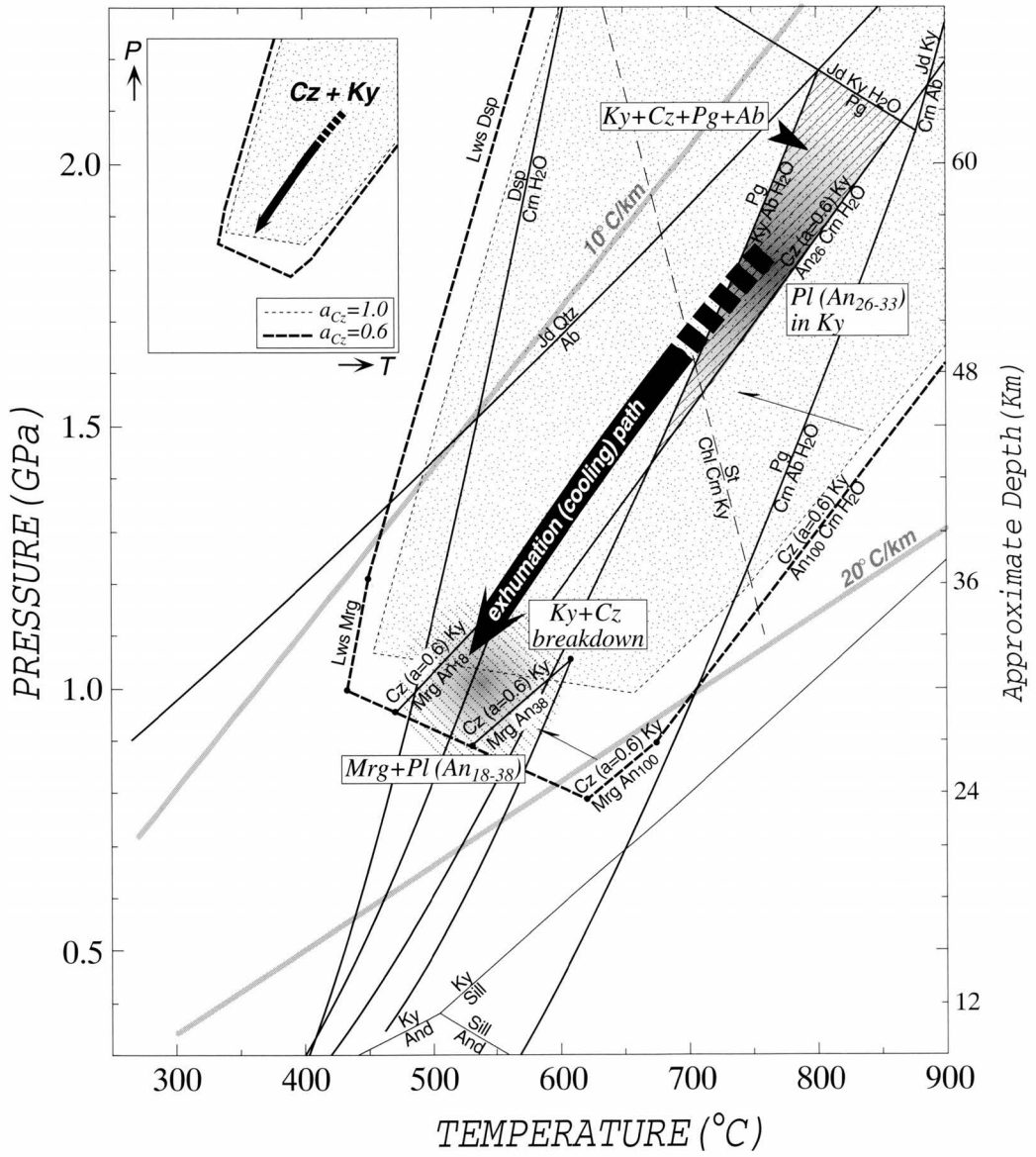

Fig. 12. Pressure-temperature diagram showing estimated metamorphic conditions (lined areas) and decompression P-T path (solid arrow) of the Fuko Pass metacumulate. The anorthite-isopleths for early stage plagioclase (An_{26}) and secondary plagioclase (An_{18-38}) define the P-T limits for the high-pressure stage and retrograde stage, respectively. The small P-T diagram showing the calculated stability fields of clinozoisite (a_{Czo} = 1.0) + kyanite and clinozoisite (a_{Czo} = 0.6) + kyanite. Staurolite-producing reaction line, which experimentally determined by Fockenberg (1998) is also presented. The approximate geothermal gradients (10°/km and 20°/km) are also drawn. Abbreviations [Qtz : quartz, Ab : albite, Pg : paragonite, Jd : jadeite, Lws : lawsonite, Mrg : margarite, Dsp : diaspor, An : anorthite, Czo : clinozoisite, Crn : corundum, Chl : chlorite, St : staurolite, Ky : kyanite ; Sill : sillimanite ; And : andalusite].

MASH (MgO-Al_2O_3-SiO_2-H_2O):

chlinochlore + kyanite + corundum = Mg-staurolite (6).

Recently, this reaction was experimentally determined and it takes place under about 2.3 GPa at 630°C and 1.1 GPa at 760°C (Fockenberg, 1998). In the foliated epidote-amphibolite, staurolite (Mg/(Mg + Fe) ratio = 0.36 at maximum) accompanies corundum, chlorite and kyanite. It is possible that the temperature condition lies on around the reaction curve (6) (Fig. 12).

Retrograde metamorphism and decompression P-T path

Retrograde P-T path is well-documented by the breakdown of the assemblage clinozoisite + kyanite to produce margarite and plagioclase by decompression. In the Fuko Pass metacumulate, the presence of Ca-bearing plagioclase (An_{18-38}) coexisting with retrograde margarite indicates a decompression P-T path passing from the clinozoisite + kyanite field through the reaction line (2). The breakdown texture of kyanite indicates that the Fuko Pass metacumulate must pass through a reaction line (2). Although the location of the reaction in the P-T space is significantly moved by the effects of solid solution, the analysed composition of secondary plagioclase ($a_{An} = X_{An}$ = 0.18 – 0.38) gives about 1.0 ± 0.1 GPa at 550 ± 50°C (Fig. 12).

The paragonite-muscovite solvus was studied by many authors (e.g. Guidotti et al., 1994). The presence of paragonite-muscovite pairs of two generations can further constrain the P-T retrogression path. The paragonite-muscovite geothermometer of Blencoe et al (1994) gives about 600°C for the inclusion pairs in the foliated epidote-amphibolite and about 480°C for the retrograde pairs in the leucocratic metagabbro. Franz et al. (1977) experimentally determined a miscibility gap in the margarite-paragonite join at 0.1 – 0.6 GPa. The solvus which exists in the region between 20 and 50 mole % margarite at 400°C narrows and is closed at about 600°C. The extremely margarite-rich paragonite occurring as inclusions in staurolite suggests a temperature higher than 600°C.

The hornblende K-Ar ages of 413 – 426 Ma of the Fuko Pass metacumulate reported by Nishina et al. (1990) may correspond to the time when the rocks passed the closure temperature (ca. 500°C) during decompression.

3. Tectonic implications

Is the Fuko Pass metacumulate unit exotic?

Kurokawa (1985) had reconstructed an ophiolitic sequence consisting of residual peridotite, ultramafic to mafic cumulate and gabbroic intrusions. If the metacumulate unit had been a part of successive sequence of the Oeyama ophiolite, the other constituent members (residual peridotite and gabbroic intrusions) should also have suffered high-pressure and moderate-temperature metamorphism together with the metacumulate unit. However, any evidence of such high-pressure and moderate-temperature metamorphism (about 1.5 – 2.1 GPa at 700 – 850°C) is observed neither in residual peridotite nor gabbroic intrusions. Such high-pressure and moderate-temperature condition is only realized at a deeper part of a subduction zone. Thus, it is interpreted that the Fuko Pass metacumulate is an exotic block which may have been trapped somehow by tectonic process.

Paleozoic metamorphic rocks associated with the Oeyama ophiolite

Some peridotite bodies of the Oeyama ophiolite in the Chugoku Mountains include tectonic block of various metamorphic rocks. A serpentinite melange containing blueschist blocks, which yield *ca.* 320 Ma phengite K-Ar ages, develops beneath a peridotite body of the Oeyama ophiolite in central Chugoku Mountains (Osayama serpentinite melange: Tsujimori, 1998; Tsujimori and Itaya, 1999). The Osayama blueschist is originated in the Renge metamorphic belt. On the other hand, Early Paleozoic amphibolite or metagabbro (highly recrystallized) occurs in eastern peridotite bodies (Kurokawa, 1985; Nishimura and Shibata, 1989; Nishina et al., 1990). Some gneissose amphibolites with 444 – 469 K-Ar hornblende age occur as tectonic blocks in the Wakasa peridotite body which tectonically overlies the Renge schist (e.g. Uemura et al., 1979). These amphibolite blocks underwent amphibolite or epidote-amphibolite facies metamorphism, and bear following mineral assemblages; hornblende + plagioclase, hornblende + clinopyroxene + plagioclase, hornblende + garnet + plagioclase and hornblende + epidote + plagioclase (Nishimura and Shibata, 1989). In the Wakasa and Izushi bodies, some coarse-grained clinopyroxenites were thoroughly recrystallized, and hornblende, clinozoisite and rutile occur as metamorphic minerals (T. Tsujimori, unpublished data). Although the critical minerals indicating high-pressure moderate-temperature mineral such as kyanite have not yet been reported, the rutile-bearing assemblage in the meta-clinopyroxenite, possibly cumulate origin, is similar to the Fuko Pass metacumulate. The metamorphism of these amphibolites associated in the Oeyama ophiolite has been considered as ocean-floor metamorphism, and their K-Ar hornblende age has been regarded as timing of the ocean-floor metamorphism (e.g. Nishimura and Shibata, 1989; Nishina et al., 1990). However, it should be interpreted as fragments of the regional metamorphic belt which have been subjected to subduction during Early Paleozoic, and then tectonically trapped into residual peridotite of the Oeyama ophiolite.

Geologic significance of the Fuko Pass high-pressure metacumulate

In southwestern Japan, the Ordovician schists of Kurosegawa belt (Maruyama and Ueda, 1974) is an evidence for an incipient subduction of the paleo-Pacific plate (e.g. Isozaki, 1996; Maruyama, 1997), although typical blueschists appear only after Devonian time as reviewed in Tsujimori and Itaya (1999). The high-pressure metamorphism preserved in the Fuko Pass metacumulate may also indicate the beginning of subduction in a paleo-Pacific margin at Early Paleozoic time.

The residual peridotite and gabbroic intrusions of the Oeyama ophiolite have been interpreted as a supra-subduction zone lithosphere possibly of primitive arc or back-arc setting (e.g. Arai and Yurimoto, 1994; Tsujimori and Itaya, 1999). It is difficult to expect high-pressure and moderate-temperature metamorphism at back-arc basin environment. The high-pressure metamorphism and the presence of relict spinel-granulite of the Fuko Pass metacumulate may suggest that the Fuko Pass metacumulate represents a fragment of subducted plutonic complex, probably lower part of an oceanic plateau, and emplaced as tectonic block into the hanging wall peridotite (present Oeyama ophiolite) after subduction. The decompression P-T path of the Fuko Pass metacumulate may imply initial subduction of a thick-crusted oceanic plateau or oceanic-arc and its subsequent exhumation.

Acknowledgments

I express sincere thanks to Dr. A. Ishiwatari for his valuable advises and critical reading of the manuscript. I am also

grateful to Professor T. Itaya for microprobe analysis at Okayama University of Science. I appreciate Dr. M. Enami of Nagoya University, who kindly gave critical suggestions for metamorphism of the Fuko Pass metacumulate. I am much indebted to Professor S. Arai, Drs. A. Toramaru, Y. Tamura and T. Morishita for their discussions. Messrs. H. Shukuno, M. Motoya and D. Saito are also thanked for their help in laboratory works. Dr. K. Kunugiza is thanked for his valuable suggestions and constructive criticisms. This study was supported financially in part by JSPS Research Fellowships for Young Scientists.

References

Ackermand, D. and Morteani, G., 1973, Occurrence and breakdown of paragonite and margarite in the Greiner Schiefer Series (Zillerthal Alps, Tyrol). *Cotnrib. Mineral. Petrol.*, **40**, 293-304.

Aitchison, J. C., Ireland, T. R. and Blake Jr., M. C. and Flood, P. G., 1992, 530 Ma zircon age for ophiolite from the New England orogen: Oldest rocks known from eastern Australia. *Geology*, **20**, 125-128.

Arai, S., 1980, Dunite-harzburgite-chromitite complexes as refractory residue in the Sangun-Yamaguchi Zone, western Japan. *Jour. Petrol.*, **21**, 141-165.

Arai, S. and Yurimoto, H., 1994, Podiform chromitites of the Tari-Misaka ultramafic complex, southwestern Japan, as mantle-melt interaction products. *Econ. Geol.*, **89**, 1279-1288.

Benoit, M., Polve, M. and Ceuleneer, G., 1996, Trace elemnt and isotopic characterization of mafic cumulates in a fossil mantle diapir (Oman ophiolite). *Chem. Geol.*, **134**, 199-214.

Blencoe, J. G., Guidotti, C. V. and Sassi, F. P., 1994, The paragonite-muscovite soluvus: II. Numerical geothermometers for natural, quasibinary paragonite-muscovite pairs. *Geochim. Cosmochim. Acta*, **58**, 2277-2288.

Chatterjee, N. D., 1976, Margarite stability and compatibility relations in the system CaO-Al_2O_3-SiO_2-H_2O as a pressure-temperature indicator. *Amer. Mineral.*, **61**, 699-709.

Chatterjee, N. D., Johannes, W. and Leistner, H., 1984, The system CaO-Al_2O_3-SiO_2-H_2O: new phase equilibria data, some caluclated phase relations, and their petrogical applications. *Contrib. Mineral. Petrol.*, **88**, 1-13.

Chopin, C., 1987, Very high-pressure metamorphism in the western Alps: implication for subduction of continental crust. *Phil. Trans. Roy. Soc. London*, **A231**, 183-197.

Cotkin, S. J., 1997, Igneous and metamorphic petrology of the eclogitic Seljeneset Meta-anorthosite and related jotunites, Western Gneiss Region, Norway. *Lithos*, **40**, 1-30.

Cotkin, S. J., Valley, J. W. and Essene, E. J., 1988, Petrology of a margarite-bearing meta-anorthite from Seljeneset, Nordfjord, western Norway: Implications for the P-T history of the Western Gneiss Region during Caledonian uplift. *Lithos*, **21**, 117-128.

Daniels, L. R. M., Gurney, J. J. and Harte, B., 1996, A crustal mineral in a mantle diamond. *Nature*, **379**, 153-156.

Efimov, A. A. and Potopova, T. A., 1992, Paragonite-clinozoisite-kyanite-quartz paragenesis as an indicator of conditions in the lower metagabbroic zone of the Voikar ophiolite allochton (Polar Urals). *Dokl. Akad. Nayk.*, **323**, 137-141. ***

Enami, M., 1980, Note on petrography and rock-forming mineralogy (8) margarite-bearing metagabbro from the Iratsu mass in the Sanbagawa belt, central Shikoku. *Jour. Mineral. Petrol. Econ. Geol.*, **75**, 245-253.

Enami, M. and Banno, S., 1980, Zoisite-clinozoisite relations in low- to medium-grade high-pressure metamorphic rocks and their implications. *Mineral. Mag.*, **43**, 1005-1013.

Enami, M. and Zang, Q., 1988, Magnesian staurolite in garnet-corundum rocks and eclogite from the Donghai district, Jiangsu province, east China. *Amer. Mineral.*, **73**, 48-56.

Fockenberg, T., 1998, An experimental investigation on the P-T stability of Mg-staurolite in the system MgO-Al_2O_3-SiO_2-H_2O. *Contrib. Mineral. Petrol.*, **130**, 187-198.

Franz, G., 1977, Determination of the miscibility gap on the solid solution series paragonite-maragrite by means of the infrared spectroscopy. *Contrib. Mineral. Petrol.*, **59**, 307-316.

Froese, E. and Hall, R. D., 1983, A reaction grod for potassium-poor pelitic and mafic rocks. *In: Current reserc (part A), Geological Survey of Canada*, Paper 83-1A, 121-124.

Frey, M., Bucher, K., Frank, E. and Schwander, H., 1982, Margarite in the central Alps. *Schweiz. Mineral. Petrogr. Mitt.*, **62**, 21-45.

Gibson, G. M., 1978, Staurolite in amphibolite and hornblendeite sheets from the Upper Seaforth River, central Fiordland, New Zealand. *Mineral. Mag.*, **42**, 153-154.

Gibson, G. M., 1979, Margarite in kyanite- and corundum-bearing anorthosite, amphibolites, and hornblendite from central Fiordland, New Zealand. *Contrib. Mineral. Petrol.*, **68**, 171-179.

Gil Ibarguchi J. I., Mendia, M. and Girardeau, J., 1991, Mg-and Cr-rich staurolite and Cr-rich kyanite in high-pressure ultrabasic rocks (Cabo Ortegal, northwestern Spain). *Amer. Mineral.*, **76**, 501-511.

Goodman, S., 1993, Survival of zincian staurolite to upper amphibolite facies metamorphic grade. *Mineral. Mag.*, **57**, 736-739.

Grapes, R. and Palmer, K., 1996, (Ruby-sapphire)-chromian mica-tourmaline rocks from Westland, New Zealand. *Jour. Petrol.*, **37**, 293-315.

Grew, E. G., Hiroi, Y. and Shiraishi, K., 1990, Hogbomite from the Prince Olav Coast, East Antarctica: An example of oxidation-exsolution of a complex magnetite solid solution? *Amer. Mineral.*, **75**, 589-600.

Grew, E. G. and Sandiford, M., 1984, A staurolite-talc assemblage in tourmaline-phlogopite-chlorite schist from northern Victori Land, Antarctica, and its petrogenetic significance. *Contrib. Mineral. Petrol.*, **87**, 337-350.

Guidotti, C. V., 1984, Micas in metamorphic rocks. In Baily, S. W., eds., *"Micas" Reviews in Mineralogy, Mineral. Soc. Amer.*, **13**, 357-467.

Guidotti, C. V., Post, J. L. and Cheney, J. T., 1979, Margarite pseudomorph after chiastolite in the Georgetown area, California. *Amer. Mineral.*, **64**, 728-732.

Guidotti, C. V., Sassi, F. P., Blencoe, J. G. and Selverstone, J., 1994, The paragonite-muscovite soluvus: I. P-T-X limits derived from the Na-K compositions of natural, quasibinary paragonite-muscovite pairs. *Geochm. Cosmochm. Acta*, **58**, 2269-2275.

Halbach, H. and Chatterjee, N. D., 1984, An internally consistent set of thermodynamic data for twentyone CaO-Al_2O_3-SiO_2-H_2O phases by linear parametric programming. *Contrib. Mineral. Petrol.*, **88**, 14-23.

Hayasaka, Y., Sugimoto, T. and Kano, T., 1995, Ophiolitic complex and metamorphic rocks in the Niimi-Katsuyama area, Okayama Prefecture. *Excurtion Guidbook of 102nd Annual Meeting of the Geological Society of Japan*, 71-87. **

Helms, T. S., McSween Jr. H. Y., Labotka, T. C. and Jarosewich, E., 1987, Petrology of a Georgia Blue Ridge amphibolite unit with hornblende + gerdrite + kyanite + staurolite. *Amer. Mineral.*, **72**, 1086-1096.

Hey, M. H., 1954, A new review of chlorites. *Mineral. Mag.*, **30**, 277-292.

Hiroi, Y., 1983, Progressive metamorphism of the Unazuki pelitic schists in the Hida terrane, central Japan. *Contrib. Mineral. Petrol.*, **82**, 334-350.

Hiroi, Y., Ogo, Y., Namba, K., 1994, Evidence for prograde metamorphic evolution of Sri Lankan pelitic granulites, and implications for the development of continental crust. *Precambrian Research*, **66**, 245-263.

Höck, V., 1974, Coexsisting phengite, paragonite and margarite in metasediments of the Mittlere Hohe Tauern, Austria. *Contrib. Mineral. Petrol.*, **43**, 261-273.

Holdaway, M. J., Dutrow, B. L. and Shore, P., 1986, A model for the crystal chemistory of staurolite. *Amer. Mineral.*, **71**, 1142-1159.

Holland, T. J. B. and Powell, R., 1990, An enlarged and unpdated internally consistent thermodynamic dataset with uncertainties

and correlations: the system K_2O-Na_2O-CaO-MgO-MnO-FeO-Fe_2O_3-Al_2O_3-TiO_2-SiO_2-C-H_2-O_2. *Jour. Metam. Geol.*, **8**, 89-124.

Ishiga, H. and Suzuki, S., 1988, Late Paleozoic radiolarian assemblages from the Shimomidani Formation in Akiyoshi Terrane, Southwest Japan. *Jour. Geol. Soc. Japan*, **94**, 493-499.

Ishiwatari, A., 1985, Igneous petrogenesis of the Yakuno ophiolite (Japan) in the context of the diversity of ophiolites *Contrib. Mineral. Petrol.*, **89**, 155-167.

Ishiwatari, A., 1990, Yakuno ophiolite and related rocks in Maizuru terrane. In K. Ichikawa et al., eds., *"Pre-Cretaceous Terranes of Japan", IGC Project 224, Osaka City University*, 109-120.

Ishiwatari, A., 1994, Circum-Pacific Phanerozoic multiple ophiolite belts. In Ishiwatari, A. et al., eds., *"Circum-Pacific Ophiolites", Proceedings of the 29th International Geological Congress*, Part D, 7-28.

Isozaki, Y., 1996, Anatomy and genesis of a subduction-related orogen: A new view of geotectonic subdivision and evolution of the Japanese Island. *The Island Arc*, **5**, 289-320.

Isozaki, Y. and Itaya, T., 1991, Pre-Jurassic klippe in northern Chichibu Belt in west-central Shikoku, Southwestern Japan: Kurosegawa Terrane as a tectonic outlier of the pre-Jurassic rocks of the Inner Zone. *Jour. Geol. Soc. Japan*, **97**, 431-450. *

Isozaki, Y. and Maruyama, S., 1991, Studies on orogeny based on plate tectonics in Japan and new geotectonic subdivision of the Japanese islands. *Jour. Geography (Tokyo)*, **100**, 697-761. *

Jenkins, D. M., 1984, Upper-pressure stability of synthetic margarite plus quartz. *Contrib. Mineral. Petrol.*, **88**, 332-339.

Kunugiza, K., Takasu, A., Banno, S., 1986, The origin and metamorphic history of the ultramafic and metagabbro bodies in the Sanbagawa metamorphic belt. *Geol. Soc. Amer. Mem.*, **164**, 375-385.

Kuroda, Y., Kurokawa, K., Uruno, K., Kinugawa, T., Kano, H. and Yamada, T., 1976, Staurolite and kyanite from epidote-hornblende rocks in the Oeyama (Komori) ultramafic mass, Kyoto Prefecture, Japan. *Earth Science (Chikyu Kagaku)*, **30**, 331-333.

Kurokawa, K., 1975, Discovery of kyanite from epidote-amphibolite in the Oeyama ultramafic mass, inner zone of southwestern Japan. *Jour. Geol. Soc. Japan*, **81**, 273-274.

Kurokawa, K., 1985, Petrology of the Oeyama ophiolitic complex in the Inner Zone of Southwest Japan. *Sci. Rept. Niigata Univ. (Series E)*, **6**, 37-113.

Kuyumjian, R. M., 1998, Kyanite-staurolite ortho-amphibolite from the Chapada region, Goias, central Brazil. *Mineral. Mag.*, **62**, 501-507.

Laird, J. and Albee, A. L., 1981, Pressure, temperature, and time indicators in mafic schist: Their application to reconstructing the polymetamorphic history of Vermont. *Amer. Jour. Sci.*, **281**, 127-175.

Lattard, D. and Bubenik, W., 1995, Synthetic staurolites in the system Mg-Fe-Al-Si-O-H. *Euro. Jour. Mineral.*, **7**, 931-947.

Leake, B. E., 1978, Nomenclature of amphiboles. *Mineral. Mag.*, **42**, 533-563.

Maruyama, S., 1997, Pacific-type orogeny revisited: Miyashiro-type orogeny proposed. *The Island Arc*, **6**, 91-120.

Maruyama, S. and Ueda, Y., 1974, Schist xenolith in ultrabasic body accompanied with Kurosegawa tectonic zone in eastern Shikoku and their K-Ar ages. *Jour. Japan. Assoc. Mineral. Petrol. Econ.*, **70**, 42-52. *

Matsumoto, I., Arai, S. and Yamauchi, H., 1997, High-Al podiform chromitites in dunite-harzburgite complexes of the Sangun zone, central Chugoku district, Southwest Japan. Jour. *Asian Earth Sci.*, **15**, 295-302.

Miller, C. and Thoni, M., 1995, Origine of eclogite from the Austroalpine Otztal basement (Tirol, Austria): geochemistry and Sm-Nd vs. Rb-Sr isotope systematics. *Chem. Geol.*, **122**, 199-225.

Minakawa, T. and Momoi, H., 1982, Ruby from the Sanbagawa metamorphic belt, in the Hodono Valley, Ehime Prefecture, Japan. *Mineral. Jour. (Japan)*, **11**, 78-83.

Morishita, T. and Kodera, T., 1998, Finding of corundum-bearing gabbro boulder possibly derived from the Horoman peridotite Complex, Hokkaido, northern Japan. *Jour. Mineral. Petrol. Econ. Geol.*, **93**, 52-63.

Moeen, S., 1991, Staurolite from a metabasite and its paragenesis. *Mineral. Mag.*, **55**, 140-142.

Nicollet, C., 1986, Saphirine et staurotide riche en magnésium et chrome dans les amphibolites et anorthosites à corindon du Vohibory Sud, Madagascar. *Bull. Mineral.*, **109**, 599-612. ****

Nishimura, Y. and Shibata, K., 1989, Modes of occurrence and K-Ar ages of metagabbroic rocks in the "Sangun metamorphic belt", Southwest Japan. *Mem. Geol. Soc. Japan*, no.33, 343-357. *

Nishina, K., Itaya, T. and Ishiwatari, A., 1990, K-Ar ages of gabbroic rocks in the "Oeyama ophiolite". *Abstracts of 97th Annual Meeting of the Geological Society of Japan.* **

Oh, C. W. and Liou, J. G., 1998, A petrogenetic grid for eclogite and related facies under high-pressure metamorphism. *The Island Arc*, **7**, 36-51.

Okuyama-Kusunose, Y., 1985, Margarite-paragonite-muscovite assemblages from the low-grade metapelites of the Tono metamorphic aureole, Kitakami Mountains, Northeast Japan. *Jour. Japan. Assoc. Min. Pet. Eco. Geol.*, **80**, 515-525.

Osanai, Y. and Owada, M., 1990, Finding of staurolite in pelitic granulites from the Hidaka metamorphic belt, Hokkaido, Japan. *Jour. Geol. Soc. Japan*, **96**, 549-552.

Perkins, D., III, Westrum Jr., E. F., and Essene, E. J., 1980, The thermodynamic properties and phase relations of some minerals in the system CaO-Al_2O_3-SiO_2-H_2O. *Geochim. Cosmochim. Acta*, **44**, 61-84.

Powell, R. and Holland, T. J. B., 1988, An internally consistent thermodynamic data set with uncertainties and correlations: 3. Application methods, worked examples and a computer program. *Jour. Metam. Geol.*, **6**, 173-204.

Prunier, A. R. Jr., and Hewitt, D. A., 1985, Experimental observations on coexsisting zoisite-clinozoisite. *Amer. Mineral.*, **70**, 375-378.

Sato, J. I. and Azanon, J. M., 1993, The breakdown of Zn-rich staurolite in a metabasites from the Betic Cordillera (SE Spein). *Mineral. Mag.*, **57**, 530-533.

Schreyer, W., 1988, Experimantal studies on metamorphism of crustal rocks under mantle pressures. *Mineral. Mag.*, **52**, 1-26.

Schreyer, W., Horrockes, P. C. and Abraham, K., 1984, High magnesium staurolite in a sapphirine-garnet rock from the LImpopo Belt, Southern Africa. *Contrib. Mineral. Petrol.*, **86**, 200-207.

Selverstone, J., Spear, F. S., Franz, G. and Morteani, G., 1984, High-presure metamorphism in the SW Tauern Window, Austria: P-T paths from hornblend-kyanite-staurolite schists. *Jour. Petrol.*, **25**, 501-531.

Shiba, M., Okamura, H. and Onuki, H., 1988, Notes on petrography and rock-forming mineralogy (18): A corundum + spinel + chrolite pseudomorph after sapphirine from the Nikanbetsu gabbro complex in the southwestern Hidaka metamorphic belt. *Jour. Mineral. Petrol. Econ. Geol.*, **83**, 289-295.

Storre, B. and Nitsch, K.-H., 1974, On the stability of margarite in system CaO-Al_2O_3-SiO_2-H_2O. *Contrib. Mineral. Petrol.*, **43**, 1-24.

Spear, F. S., 1982, Phase equilibria of amphibolites from the Post Pond Volcanics, Mt. Cube Quadrangle, Vermont. *Jour. Petrol.*, **25**, 383-426.

Tenrhorey, E. A., Ryan, J. G. and Snow, E. A., 1996, Petrogenesis of sapphirine-bearing metatroctolites from the Buck Creek ultramafic body, southern Appalachians. *Jour. Metam. Geol.*, **14**, 103-114.

Tindle, A. G. and Webb, P. C., 1994, PROBE-AMPH-a spreadseet program to classify microprobe-derived amphibole analyses. *Computers and Geoscience*, **20**, 1201-1228.

Tsujimori, T., 1995, Staurolite-bearing sillimanite schist cobble from the Upper Jurassic Tetori Group in the Kuzuryu area, Hida Mountains, central Japan. *Jour. Geol. Soc. Japan*, **101**, 971-977.

Tsujimori, T., 1998, Geology of the Osayama serpentinite melange in the central Chugoku Mountains, southwestern Japan: 320 Ma blueschist-bearing serpentinite melange beneath the Oeyama ophiolite. *Jour. Geol. Soc. Japan*, 104, 213-231.*

Tsujimori, T., Esaka, N., Abimbola, A. F., Nishido, H., Ninagawa, K. and Itaya, T., 1997, Quantitative analysis of common rock-forming minerals by a modern wavelength-dispersive type EPMA: A preliminary report. *Bull. Research Institute of Natural Sciences, Okayama University of Science*, 23, 51-60.

Tsujimori, T. and Ishiwatari, A., 1998, Granulite-facies relics in high-pressure metacumulate of Oeyama ophiolite: evidence for isobaric cooling beneath 35km. *Abstracts of 1998 Japan Earth and Planetary Science Joint Meeting.***.

Tsujimori, T. and Itaya, T., 1999, Blueschist-facies metamorphism during Paleozoic orogeny in southwestern Japan: phengite K-Ar ages of blueschist-facies tectonic blocks in a serpentinite melange beneath Early Paleozoic Oeyama ophiolite. *The Island Arc*, 8, 190-205.

Uemura, F., Sakamoto, T. and Yamada, N., 1979, Geology of the Wakasa district. *Quadrangle Series, Scale 1: 50,000*. Geological Survey of Japan.*

Uda, S., 1984, The contact metamorphism of the Oeyama ultrabasic mass and the genesis of the "cleavable olivine" *Jour. Geol. Soc. Japan*, 90, 393-410.*

Wallin, E. T., Mattinson, J. M. and Potter, A. W., 1988, Early Paleozoic magmatisc events in the eastern Klamath Mountains, northern California. *Geology*, 16, 144-148.

Ward, C. M., 1984, Magnesium staurolite and green chromian staurolite from Fiordland, New Zealand. *Amer. Mineral.*, 69, 531-540.

Yokoyama, K., 1980, Nikubuchi peridotite body in the Sanbagawa metamorphic belt; thermal history of the 'Al-pyroxene-rich suite' peridotite body in high pressure metamorphic terrain. *Contrib. Mineral. Petrol.*, 73, 1-13.

Yokoyama, K. and Goto, A., 1987, Mg-rich staurolite from the Iratsu epidote amphibolite body, central Shikoku. *Jour. Japan. Assoc. Min. Pet. Eco. Geol.*, 82, 281-290.

* in Japanese with English abstract
** in Japanese
*** in Russian
**** in French with English abstract

(要　旨)

Tsujimori, T., 1999, Petrogenesis of the Fuko Pass high-pressure metacumulate block from the Oeyama peridotite body, southwestern Japan: evidence for Early Paleozoic subduction metamorphism. *Mem. Geol. Soc. Japan*, no. 52, 287-302（辻森　樹，1999，大江山かんらん岩体に産する普甲峠高圧変成沈積岩体の岩石学的成因：古生代前期の沈み込み変成作用の証拠，地質学論集，第52号，287-302.）

京都府北部，大江山かんらん岩体に産する藍晶石や十字石を含む変成沈積岩ユニット（普甲峠高圧変成沈積岩体）の地球化学的特徴及び変成作用・変成経路を明らかにした．全岩化学組成及び計算されたノルム鉱物は，灰長石に富み非常に分化したトロクトライト的な深成岩体の一部であったことを示唆する．普甲峠高圧変成沈積岩体はホルンブレンド＋クリノゾイサイト（＋ゾイザイト）＋藍晶石（An_{26-33}の斜長石包有物を含む）＋パラゴナイト±マスコバイト＋緑泥石＋曹長石±十字石±コランダム＋ルチル±イルメナイトの鉱物組み合わせで特徴づけられ，藍晶石＋パラゴナイト＋曹長石＋クリノゾイサイトの共生関係から約1.5～2.1 GPa，700～850 ℃の高圧中温の変成条件が推定される．また，二次的な産状のマーガライト，パラゴナイト（±マスコバイト），斜長石（An_{18-38}），緑泥石が藍晶石を置換する．藍晶石とクリノゾイサイトの分解反応によるマーガライトと斜長石の形成は，減圧（上昇）のP-T経路を示す．これまで，この変成沈積岩体は大江山オフィオライトの層序の一部と考えられてきたが，その岩石学的な特徴から大江山かんらん岩体とは履歴の異なる古生代前期高圧型広域変成岩の異質ブロックであって，構造的にかんらん岩体に取り込まれたものであろう．